AD-A136 415 DEVELOPMENT OF FATIGUE AND CRACK PROPAGATION DESIGN AND 1/1
ANALYSIS METHODOL..(U) GENERAL DYNAMICS FORT WORTH TX
FORT WORTH DIV Y H KIM ET AL. MAR 83
UNCLASSIFIED NADC-83126-60-VOL-2 N62269-81-C-0268 F/G 20/11 NL

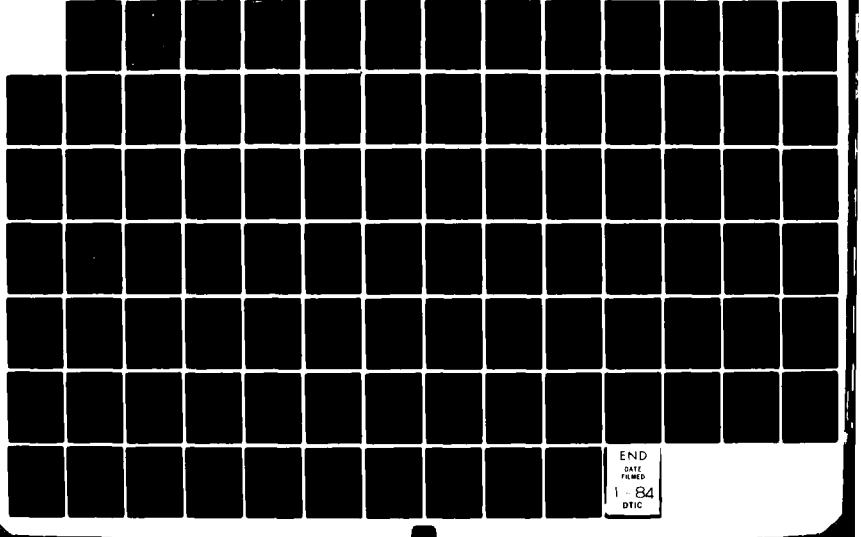

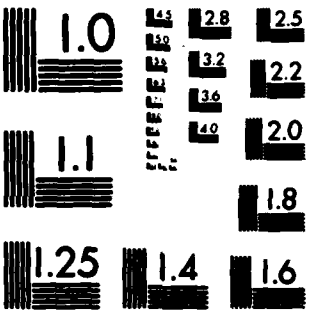

MICROCOPY RESOLUTION TEST CHART
NATIONAL BUREAU OF STANDARDS-1963-A

REPORT NO. NADC-83126-60 Vol.II

DEVELOPMENT OF FATIGUE AND CRACK PROPAGATION DESIGN AND ANALYSIS METHODOLOGY IN A CORROSIVE ENVIRONMENT FOR TYPICAL MECHANICALLY-FASTENED JOINTS VOLUME II - STATE-OF-THE-ART ASSESSMENT

A136415

Y. H. Kim
S. M. Speaker
S. D. Manning
STRUCTURES AND DESIGN DEPARTMENT
GENERAL DYNAMICS FORT WORTH DIVISION
P.O. Box 748
Fort Worth, Texas 76101
and
R. P. Wei
LEHIGH UNIVERSITY
Bethlehem, PA 18015

DEC 2 8 1983
A

MARCH 1983

Final Report for Period May 1981 - September 1982

DTIC FILE COPY

Approved for Public Release; Distribution Unlimited

Prepared For
Department of the Navy
NAVAL AIR DEVELOPMENT CENTER
Warminster, PA 18974

83 12 28 010

Unclassified

SECURITY CLASSIFICATION OF THIS PAGE (When Data Entered)

REPORT DOCUMENTATION PAGE		READ INSTRUCTIONS BEFORE COMPLETING FORM
1. REPORT NUMBER NADC-83126-60 Vol. II	2. GOVT ACCESSION NO. AD-A136	3. RECIPIENT'S CATALOG NUMBER 415
4. TITLE (and Subtitle) Development of Fatigue and Crack Propagation Design and Analysis Methodology in a Corrosive Environment for Typical Mechanically Fastened Joints Vol. II - State-of-the-Art Assessment		5. TYPE OF REPORT & PERIOD COVERED Final Report May 1981 - September 1982 6. PERFORMING ORG. REPORT NUMBER
7. AUTHOR(s) Y. H. Kim, S. M. Speaker, R. P. Wei, S. D. Manning		8. CONTRACT OR GRANT NUMBER(s) N62269-81-C-0268
9. PERFORMING ORGANIZATION NAME AND ADDRESS General Dynamics Fort Worth Division P. O. Box 748, Fort Worth, TX 76101		10. PROGRAM ELEMENT, PROJECT, TASK AREA & WORK UNIT NUMBERS 62241N WF 41400, ZA-61A
11. CONTROLLING OFFICE NAME AND ADDRESS Naval Air Development Center (NADC) Warminster, PA 18974		12. REPORT DATE March 1983 13. NUMBER OF PAGES 73
14. MONITORING AGENCY NAME & ADDRESS(if different from Controlling Office)		15. SECURITY CLASS. (of this report) Unclassified 15a. DECLASSIFICATION/DOWNGRADING SCHEDULE

16. DISTRIBUTION STATEMENT (of this Report)

Approved for public release; distribution unlimited.

17. DISTRIBUTION STATEMENT (of the abstract entered in Block 20, if different from Report)

18. SUPPLEMENTARY NOTES

The subcontractor/consultant for this report was R. P. Wei, Lehigh University, Bethlehem, PA 18015

19. KEY WORDS (Continue on reverse side if necessary and identify by block number)

Corrosion Fatigue, Crack Initiation, Crack Propagation, Corrosive Environments

20. ABSTRACT (Continue on reverse side if necessary and identify by block number)

Navy corrosion fatigue design requirements for metallic airframes and general design practices for satisfying these requirements are briefly reviewed. The phenomenon of and mechanisms responsible for corrosion fatigue crack initiation are reviewed. The mechanisms discussed include the stress-concentration pit mechanism, the film rupture mechanism, and the preferential dissolution mechanism. Two fracture mechanics models are described and discussed (Continued)

DD FORM 1 JAN 73 1473 EDITION OF 1 NOV 65 IS OBSOLETE

Unclassified

SECURITY CLASSIFICATION OF THIS PAGE (When Data Entered)

20. Abstract (Continued)

for quantitatively predicting the number of cycles to corrosion fatigue crack initiation: (1) stress-initiation life model and (2) strain-initiation life model. Methods are also discussed for using these initiation models for spectrum loading applications. Corrosion fatigue crack propagation mechanisms are reviewed and existing models are critiqued. Propagation models evaluated include a surface reaction controlled model, a transport controlled model, and a diffusion controlled model. These models recognize hydrogen embrittlement as the overwhelming cause of corrosion fatigue propagation enhancement. Models for load-environment interaction are described and discussed, including the generalized Wheeler model, the generalized Willenborg model, the generalized Closure model and the Vroman/Chang model.

Accession for
NTIS GRA&I
DTIC TAB
Unannounced
Justification
By
Distribution/
Availability Codes
Dist | Avail and/or Special
A-1

DTIC COPY INSPECTED

FOREWORD

This program is conducted by General Dynamics Fort Worth Division (GD/FWD), with Lehigh University (Prof. R. P. Wei) as subcontractor/consultant. This report was prepared under Contract No. N62269-81-C-0268. The program is sponsored by the Naval Air Development Center, Warminster, PA, with Dr. E. Lee and Mr. P. Kozel as the project engineers. M. S. Rosenfeld of NADC initiated the program. Dr. S. D. Manning and Dr. Y. H. Kim of General Dynamics' Materials Research Laboratory are the Program Manager and Principal Investigator, respectively. S. M. Speaker of the GD/FWD supported the documentation for this Volume (II).

Phase I is documented in two volumes as follows:

Vol. I - Phase I Documentation

Vol. II - Corrosion Fatigue State-of-the-Art Assessment

This report documents the work performed under Phase I, Task 1 - Methodology and Data State-of-the-Art Assessment.

THIS PAGE INTENTIONALLY LEFT BLANK

TABLE OF CONTENTS

TABLE OF CONTENTS (Continued)

LIST OF ILLUSTRATIONS

THIS PAGE INTENTIONALLY LEFT BLANK

LIST OF SYMBOLS

a = Radius of elliptical hole in the major axis

a_0 = Crack initiation crack size

A = Empirical constant determined from plot of log N_i versus log $(\Delta\sigma_{eff}^2 - \Delta\sigma_{th}^2)$

b = Radius of elliptical hole in the minor axis or fatigue-strength exponent

B = Fatigue-strength exponent or $\Delta\sigma_{th}^2$

C = Fatigue-ductility exponent or $N_i\Delta\sigma^2$

CF = Corrosion fatigue

D = Diffusivity of Hydrogen

$(\frac{da}{dN})_e$ = Rate of fatigue crack growth in an aggressive environment

$(\frac{da}{dN})_{cf}$ = Cycle-dependent corrosion fatigue crack growth rate

$(\frac{da}{dN})_{cf} = \left[(\frac{da}{dN})^*_{cf,s} - (\frac{da}{dN})_r\right]\phi$

$(\frac{da}{dN})^*_{cf,s}$ = Cycle-dependent rate of "pure" corrosion fatigue crack growth

$(\frac{da}{dN})_{cf,s}$ = Saturation fatigue crack growth rate for the transport and surface reaction controlled case

$(\frac{da}{dN})_r$ = Rate of fatigue crack growth in an inert environment

$(\frac{da}{dN})_{scc}$ = Contribution of sustained-load crack growth (i.e., by stress corrosion cracking) at K levels above K_{Iscc}

LIST OF SYMBOLS (Continued)

E = Elastic modulus or error

E_d = Activation energy for hydrogen diffusion

f = Cyclic load frequency

G_B = Binding energy of hydrogen atoms to a dislocation

k = Boltzmann's constant

k_c = Reaction rate constant

K_I = Stress intensity factor

K_{I_c} = Critical stress intensity factor for static loading and plane strain conditions or plane-strain fracture toughness

K_{Iscc} = Plane strain stress intensity threshold below which subcritical cracks will not propagate under static loading

K_Q = Tentative value of plane strain fracture toughness

K_t = Elastic stress concentration factor

LCF = Low cycle fatigue

M = Molecular weight of the gas

n' = Cyclic work hardening exponent

N_f = Number of cycles to failure

N_i = Number of cycles to fatigue crack initiation

N_o = Density of surface sites

p = Pressure at the crack tip

P_o = Pressure of gas in surrounding environment

LIST OF SYMBOLS (Continued)

R = Stress ratio or gas constant

t = Time

T = Absolute temperature

U_{CRIT} = Critical energy for fatigue crack initiation

$\bar{X}$ = Mean

Z = No. of standard deviations from the mean

α, β^* = Empirical constant for surface roughness and gas flow, respectively

σ'_f = Fatigue-strength coefficient

σ_{ys} = Yield strength of the material

σ'_o = Cyclic yield stress

$\sigma(\bar{X})$ = Standard deviation for $\bar{x}$

$\Delta\sigma$ = Stress range

$\Delta\sigma_{eff}$ = Effective stress range = $\sigma_{max} - \sigma_{min}$ where load sequence or load interaction does not occur

$\Delta\sigma_{th}$ = Threshold stress for crack initiation corresponding to the fatigue limit

$\Delta\sigma_{rms}$ = Root mean squared $\Delta\sigma$ = $\sqrt{\frac{\sum_{i=1}^{k} \Delta\sigma_i^2}{n}}$

$\Delta\varepsilon_{rms}$ = Root mean squared $\Delta\epsilon$ = $\sqrt{\frac{\sum_{i=1}^{k} \Delta\varepsilon_i^2}{n}}$

LIST OF SYMBOLS (Continued)

ε_f' = Fatigue-ductility coefficient

$\Delta\varepsilon$ = Total strain range

$\Delta\varepsilon_e$ = Elastic strain range

$\Delta\varepsilon_p$ = Plastic strain range

ΔK = Range of stress intensity factor

ϕ = Areal fraction for corrosion fatigue

ν = Poisson's ratio

SUMMARY

The groundwork needed to develop a mechanistic-based corrosion fatigue analysis methodology for mechanically fastened joints is documented in this report. This effort was necessary to assure that the corrosion fatigue methodology to be developed would be responsive to Navy aircraft design requirements and to consolidate the existing corrosion fatigue technology for further development.

Navy corrosion fatigue design requirements for metallic airframes and general design practices for satisfying these requirements are reviewed and discussed. A critical review of existing corrosion fatigue models for crack initiation and for crack propagation is made to determine their effectiveness and potential. Current understanding of corrosion fatigue mechanisms and significant variables are also investigated. Methods are also discussed for extending the crack initiation and the crack propagation models to spectrum loading applications.

Based on this investigation, it was concluded that:

1. Current corrosion fatigue analysis tools, methodology and design data are inadequate to confidently demonstrate

aircraft structural design compliance with Navy design requirements.

2. The corrosion fatigue analysis methodology for crack initiation and for crack propagation should be developed and evaluated for mechanically-fastened joints considering at least the following variables: environment, load spectrum, stress level, R-ratio loading frequency, and holding time.

3. The stress-initiation life and the strain-initiation life models are promising for predicting corrosion fatigue crack initiation under constant amplitude loading. Further work is required to extend the models to spectrum loading.

4. Hydrogen embrittlement is the primary cause of corrosion fatigue propagation enhancement.

5. The following mechanistic-based models are promising for predicting the cycle-dependent component of corrosion fatigue crack propagation: transport-controlled model, surface-reaction-controlled model and diffusion-controlled model. These models need to be further evaluated using the experimental data to be acquired under this program.

6. The corrosion fatigue behavior of titanium alloys is very complex. Therefore, a better understanding of corrosion fatigue mechanisms may be required before a reliable corrosion fatigue analysis methodology can be developed for titanium alloys.

THIS PAGE INTENTIONALLY LEFT BLANK

SECTION I

INTRODUCTION

According to current Navy specifications [1-11] aircraft structure must be designed for strength, stiffness and life. The design must account for the effects of the expected operating environment and service load spectra - consistent with the planned aircraft usage. Corrosion fatigue is recognized as one of the most important aspects of aircraft structural design. However, it is difficult to demonstrate compliance with Navy design specifications for several reasons:

1. Difficult to realistically define actual in-service environment and load spectra.

2. What corrosion fatigue tests should be conducted to acquire reliable design data that will be applicable to the expected in-service environment and usage?

3. Several variables affect corrosion fatigue (e.g., environment, stress level, R ratio, loading frequency, waveform, holding-time, etc.) and the effects of such variables may vary depending on the material. What are the

most significant corrosion fatigue variables and how should they be accounted for in the testing and the analytical methodology?

4. Reliable mechanistic-based analytical tools for predicting crack initiation and crack propagation in a corrosive environment are lacking.

Fatigue cracking in fastener holes is one of the most prevalent forms of damage occurring in in-service aircraft and a primary site for corrosion-related problems. For this reason, the main objective of the current corrosion fatigue program is to develop and verify analytical methodology for predicting the time-to-crack-initiation and time-to-failure for mechanically-fastened joints in a corrosive environment.

This report provides the initial groundwork for developing a mechanistic-based corrosion fatigue analysis methodology that will be responsive to Navy design requirements. Navy structural design requirements and practices are reviewed and discussed in Section II. A corrosion fatigue state-of-the-art review for crack initiation and for crack propagation is documented in Sections III and IV, respectively. Corrosion fatigue variables and mechanisms are examined in detail. Conclusions for this investigation are summaried in Section V.

SECTION II

NAVY STRUCTURAL DESIGN REQUIREMENTS AND PRACTICES

2.1 INTRODUCTION

Navy structural design requirements for metallic airframes are briefly discussed in this section in terms of corrosion fatigue and crack propagation considerations. In addition, the shortcomings of existing design practices for satisfying the Navy's requirements and the problem of accounting for the effects of environment on structural design are discussed. This section puts into perspective the corrosion fatigue problem in view of the present program goals.

2.2 NAVY STRUCTURAL DESIGN REQUIREMENTS AND PRACTICES

Current Navy general requirements for aircraft design, construction, and structural integrity are described in SD-24K (Volume 1) [1] and MIL-A-8860 [2]. Specific requirements for loads/environment, strength fatigue, rigidity, design verification, and reporting are documented in the MIL-A-8861 through MIL-A-8870 series specifications [4-11].

The current Navy specification for strength and rigidity, MIL-A-08860, specifies that the operating environment consistent with overall planned usage and the effects of the operating environment on the residual physical properties of materials must be considered in the determination of allowable strength for design purposes. Although corrosion fatigue is recognized as one of the most important causes of failure in Naval aircraft, it is quite difficult to demonstrate compliance with these specifications. Problems in demonstrating compliance stem primarily from inadequate analytical methods for predicting fatigue life based on the use of full-scale fatigue tests for determining structural reliability. However, the testing of full-scale structure is too limited to obtain statistically valid experimental data because of the cost and excessive time required for performing tests. Therefore, laboratory simulated tests are usually performed on inexpensive and simple structures that contain the basic constructional characteristics of full-scale structures in corrosive environments.

The current methodology for Naval aircraft design and verification of structural integrity has been quite successful in many respects. For example, to date no losses of F-14 aircraft have been attributable to structural

failure. Indeed, Navy design requirements are built around a philosophy that the number of permissible aircraft losses due to structural failure shall be exactly zero. Additionally, recent aircraft programs have made great strides in eliminating obviously unsatisfactory design concepts, materials, and fabrication practices which have been shown to be notoriously susceptible to corrosion, stress-corrosion cracking, and/or corrosion fatigue. The active involvement of "corrosion control design teams" in programs such as the F-14, F-16 and F-18, provide a process by which aircraft hardware can be analyzed at each stage from preproduction through service introduction and beyond. In so doing, corrosion-prone locations can be identified and corrected early in the program effort.

Nevertheless, as an aircraft ages, fatigue damage accumulates at stress concentrations, and the effectiveness of the corrosion preventive finish system degrades despite periodic rework. These conditions lead to a dramatic rise in the maintenance required to repair parts cracked by corrosion fatigue during the later portion of an aircraft's service life. Corrosion fatigue problems such as these are seldom predictable based upon results of the initial fatigue test article programs. Such test programs are conducted in lab air and simulate the loading experienced by an airframe

over two design lifetimes. The main reason for testing in excess of the expected design life is to account for the environmental factor. However, the specified test duration is generally a uniform requirement regardless of the fact that some parts on an aircraft will be exposed to a more severe environment in service than others. This verification practice penalizes those parts which will be more protected from the environment, while those that are in more exposed locations may be underdesigned and ultimately become a maintenance problem. While MIL-A-8860 may require that influence of the anticipated environmental exposure on fatigue life be considered, the designer is poorly equipped to address this requirement properly. The anticipated environmental exposure profile is rarely defined, furthermore, there are no specified requirements. Even if they were available, the existing data base on material behavior for both complex spectrum loading and load-environment interaction is insufficient in nearly all cases.

No designer has ever felt comfortable with the task of devising a "fix" for either a corrosion fatigue service problem or a fatigue test article failure, since a high level of assurance that the problem will not recur is usually demanded and only a minimum time period is available to demonstrate that the "fix" will work. If corrosion

fatigue behavior of materials were sufficiently well understood, an alloy or temper change might be made with confidence. However, the usual solution at present is to "beef-up" the part and accept a weight penalty. Service life extension analysis is another area where problems arise due to uncertainty in corrosion fatigue analysis. It depends upon an accurate assessment of service history and accumulated damage to predict the remaining life and recommend repairs to extend life.

Airframe designers are faced with many uncertainties in trying to account for load-environment interactions while minimizing unnecessary penalties in structural weight. Because of the large number of variables which must be considered, the coupon testing required to generate a complete design data base is expensive and time consuming. A partial solution would be to conduct the full scale and article fatigue testing in a simulated naval environment rather than lab air, but such tests would rarely be either practical or feasible. Nor can a designer expect to be consistently successful by identifying and using component designs which have worked in the past because of the major differences at the detail level from one aircraft to another. Therefore, the only reasonable approach is to provide the structural designer with the tools necessary for

confident prediction of fatigue life under specified loading and environmental conditions.

Navy requirements for both fatigue life and damage tolerance [1,2,7] entail different philosophies and analysis considerations. For example, for fatigue analysis purposes, the Navy assumes that no flaws exist initially in the structure other than those inherent flaws produced by manufacturing. The Navy uses conventional fatigue analysis methods: (1) to assure that the airframe design will equal or exceed the specified service life, and (2) to evaluate in-service maintenance requirements.

Contractors perform fatigue analyses to analytically demonstrate that the aircraft structure will equal or exceed the design service life. Such analyses are used to establish a suitable initial design, to evaluate fatigue test failures and to assess equivalent fatigue damage resulting from changes in usage or design.

Fatigue analysis details may vary from contractor to contractor, but the essential features of the fatigue analysis approach are typified by the following approach used by the Grumman Aerospace Corporation [14]:

- Fatigue properties of the material at the root of a notch, or other stress raiser, are the same as those found from tests of unnotched specimens of the same material.

- The effects of the stress or strain history of the root material, including the effects of residual stresses due to high load applications, are considered in the analysis.

- Fatigue damage at the notch root is determined by using the Manson strain cycling principle [15]. The strain history at the notch root is correlated to the surrounding stress field, Stowell's strain concentration formula [16], and the elastic stress concentration factor. Neuber's notch sensitivity factor is commonly used [17].

- Miner's rule is used to predict the cumulative fatigue damage caused by the applicable load spectra.

Coupon specimens with holes or other stress raisers are used to generate the S-N data needed to implement Miner's cumulative damage rule. Constant amplitude tests are

performed at selected stress levels, stress ratios, and stress concentrations.

The full-scale fatigue test is typically performed using a conservative repeated load spectra. According to MIL-A-8867, the full-scale fatigue test must demonstrate a fatigue life equal to or greater than twice the design service life. Results of the fatigue test are correlated with results obtained from fatigue damage monitoring systems of in-service aircraft. A transfer function is developed to relate the cumulative damage predictions to the fatigue test results and in turn to the in-service damage monitoring data. Analytical predictions are made to establish intervals for structural maintenance, repairs and/or replacements.

Navy damage tolerance requirements are loosely defined in SD-24K (Volume 1), which simply states that the aircraft structure must be designed for both damage tolerance and fatigue life. The purpose of the damage tolerance requirements is to assure that undetected flaws or specified damage in the structure will not cause a failure in service before the damage can be detected and appropriate action taken to ensure aircraft structural integrity (e.g., repair or replacement).

The allowable sizes of initial flaws to be used for damage tolerance analyses are negotiated between the contractor and the Navy. Contractors usually develop a damage tolerance assessment plan, including rationale for crack initiation and/or initial flaw sizes. This plan is then submitted to the Navy for approval and/or revisions.

Coupon specimens and constant amplitude tests are used to generate crack growth data needed to analyze damage tolerance. Crack growth properties are usually determined for a baseline environment (e.g., dry air) and for an aggressive environment (e.g., 3.5% NaCl solution). Test results are used to determine crack growth rates (da/dN) as a function of stress intensity factor range, ΔK.

A deterministic crack growth approach based on fracture mechanics principles is commonly used. The input parameters for a given crack growth increment are constant, resulting in a single value prediction. Cumulative crack growth is determined by summing the crack growth increments. The following information is required to implement the crack growth analysis:

- Initial flaw size and shape

- Crack growth law for computing the crack growth increment

- Retardation model, which accounts for load sequence effects

- Cycle counting scheme for converting flight-by-flight load spectra into equivalent constant amplitude cycles

- Log da/dN versus log ΔK plot for applicable material and environment.

A critical crack size is defined on the basis of the material fracture toughness, crack geometry, and stress level.

Existing analytical procedures are inadequate for quantitatively estimating the corrosion fatigue life of structural components in the design stage or for quantitatively assessing and analyzing the impact of a particular corrosion fatigue service failure. Without the tools to make these quantitative predictions, the airframe contractor has no method to demonstrate compliance with design requirements that specify a level of structural durability, or that seek to assure the structural integrity

of fracture-critical parts for the expected service life, loading and environment. Furthermore, without methods to demonstrate compliance, rigorous design requirements cannot be properly established.

The corrosion fatigue methodology to be developed under the present program will provide a state-of-the-art advancement in prediction tools. Also, the results of this program will provide the framework for making further advances in the development of corrosion fatigue methodology.

THIS PAGE INTENTIONALLY LEFT BLANK

SECTION III

CORROSION FATIGUE CRACK INITIATION

3.1 INTRODUCTION

It is well known that in most fatigue loading, including spectrum loading, the greatest portion of fatigue life is spent in the initiation and growth of microcracks (usually defined as fatigue crack initiation). On the practical side, this process is quite important, especially for blunt notches such as drilled holes. Furthermore, this process has been known to be fundamentally and phenomenologically quite different from the macrocrack propagation usually occurring perpendicular to the loading direction. Thus, linear elastic fracture mechanics approaches could not have been successfully applied to fatigue crack initiation phenomena.

The increasing importance of understanding the fatigue behavior of materials has prompted much interest in the separate approach of initiation and propagation. This separation has provided better definition and focus, and has been beneficial in terms of developing a life prediction methodology. A substantial amount of "propagation" work has

been directed at quantitative modeling, limited modeling work for "initiation" is available to date. Quantitative characterization and understanding for initiation have been hampered by the complexity of the phenomenon, lack of understanding, and the inadequate body of available experimental data. Therefore, the state-of-the-art review will primarily deal with the mechanism of the initiation process in this section. The modeling work for initiation will be described briefly in subsection 3.3. The discussion in subsection 3.2 will be restricted to phenomenological understanding of corrosion fatigue crack initiation.

3.2 STATE-OF-THE-ART REVIEW

Many earlier investigators [18-22] disagreed about the effect of gaseous environments on the fatigue crack initiation phenomenon of metals. However, it was widely agreed that the effect of an aggressive environment on initiation was generally less than on propagation. Several investigators [23-27] found that the fatigue crack initiation process occurred from prominent slip band (PSB) formation and that this slip-step formation was enhanced in an aggressive environment. For example, Thompson [23] postulated that cyclically induced slip bands become regions

of high oxygen concentration because of strain-induced oxygen generation. Dissolved oxygen then prevents initial rewelding of developing cracks and accelerates the transition from slip band to microcrack, thus resulting in early crack initiation in a corrosive environment. This theory was later supported by Bennett's observation [28] that water vapor accelerated the oxidation of emerging slip bands in aluminum, thus blocking reverse slip. Shen et al. [29] also attributed their observations of early initiation to the fact that metal and alloy surfaces are strengthened by an oxide film, and subsequently, dislocations are accumulated in the surface region, enhancing the formation of cavities and voids.

On the other hand, Snowden [30,31] found that fatigue cracks in some materials (such as lead) initiated intergranularly in air and transgranularly in vacuum. He attributed this occurrence to a reduction of grain boundary energy by absorbed oxygen from the atmosphere. Broom and Nicholson [18] also postulated that water vapor dissociates to form hydrogen, which embrittles aluminum alloys and causes premature cracking. Yet, some investigators claimed that gaseous environments had little or no effect on initiation [20-22, 32-35], depending upon material-environment systems.

The effect of aqueous environments on crack initiation has been studied extensively [e.g., 36-40]. In general, most researchers agree that aqueous environments do affect initiation; however, they do not agree on the mechanisms involved. These mechanisms can be summarized as follows:

- o Stress concentrations at the bases of hemispherical pits created by the corrosive environment (stress-concentration pit mechanism)

- o Electrochemical attack at ruptures in an otherwise protective surface film (film rupture mechanism)

- o Electrochemical attack at plastically-deformed areas, with non-deformed metal acting as a cathode (electrochemical dissolution mechanism)

3.2.1 Stress-Concentration Pit Mechanism

Many earlier investigators [41-46] favored the stress-concentration pit mechanism, because observation of fracture surfaces revealed numerous cracks emanating from hemispherical pits on the metal surface. Pitting of fracture surfaces undoubtedly leads to a reduction in

fatigue life; however, some materials have been shown to be highly susceptible to some environments where pitting does not occur [45,46]. Duquette and Uhlig [47] examined low carbon steel fatigue-loaded in 3% NaCl solutions and concluded that no cracking could be attributed to the presence of hemispherical pits. They observed crystallographically-oriented pitting on the specimen surface, yet did not see any fatigue cracks emanating from the pits. The maximum extent of observed initiated cracks was equivalent to the depth of the pits with no normal fatigue cracks associated with the pits. Thus, they concluded that the pits are a result of corrosion fatigue cracking rather than a cause.

3.2.2 Film-Rupture Mechanism

Simnad and Evans [45,48] proposed a surface film rupture mechanism for initiation, which has been supported by others [49,50]. This mechanism involves fatigue steps breaking a covering surface film thus exposing anodic regions to large regions of the cathodic film. Spahn [51,52], however found that some materials could be anodically protected from corrosion fatigue in buffered acidic solutions; the protective film apparently does not affect initiation. This finding led Laird and Duquette [53] to the conclusion that

even in instances in which cathodic films are present, either the stresses are not sufficient to rupture the surface films or slip band emerges at a low enough rate that film repair takes place more rapidly than does significant corrosion damage due to a galvanic couple between emerging metal and film.

3.2.3 Electrochemical Dissolution Mechanism

Whitman and Evans [54] later suggested that failure is caused by distorted metal acting as anode and undistorted metal acting as cathode. They further postulated that very fine microcracks advanced by a combination of electrochemical and mechanical action. This mechanism seems to be the most promising because it relates to a phenomenological understanding of initiation due to load and environment interaction [54-59]. During cyclic loading, fatigue cracks usually initiate at or near singularities on or near metal surfaces. Such singularities may be coarse particles or inclusions, embrittled grain boundaries, sharp scratches, pits or slip bands depending upon microstructure, material and manufacturing quality [60-62].

Based on the observations of many previous investigators and the mechanisms described above, the following phenomena

are suggested for fatigue crack initiation in a corrosion environment [55,56,63]:

- o Persistent slip bands are preferentially attacked, leading to stress intensification and subsequent early crack initiation.

- o Corrosion results in a significant increase in the density of persistent slip bands, which produce numerous crack initiation sites.

In summary, the mechanical force from cyclic loads generates the to-and-fro motion of dislocation along slip planes, leading to slip steps and microcrack initiation [60-62,64,65]. Additionally, the preferential electrochemical attack on the predominant slip planes accelerates the process of crack nucleation [45,54-56]. This phenomenon, schematically illustrated in Fig. 1, implies that the micromechanisms and electrochemical potential should be considered for corrosive fatigue crack initiation methodology. From this viewpoint, the model and methodology for predicting corrosion fatigue crack initiation life must be developed on the basis of interaction of two driving forces; cyclic mechanical force and electrochemical potential.

INITIATION PROCESS

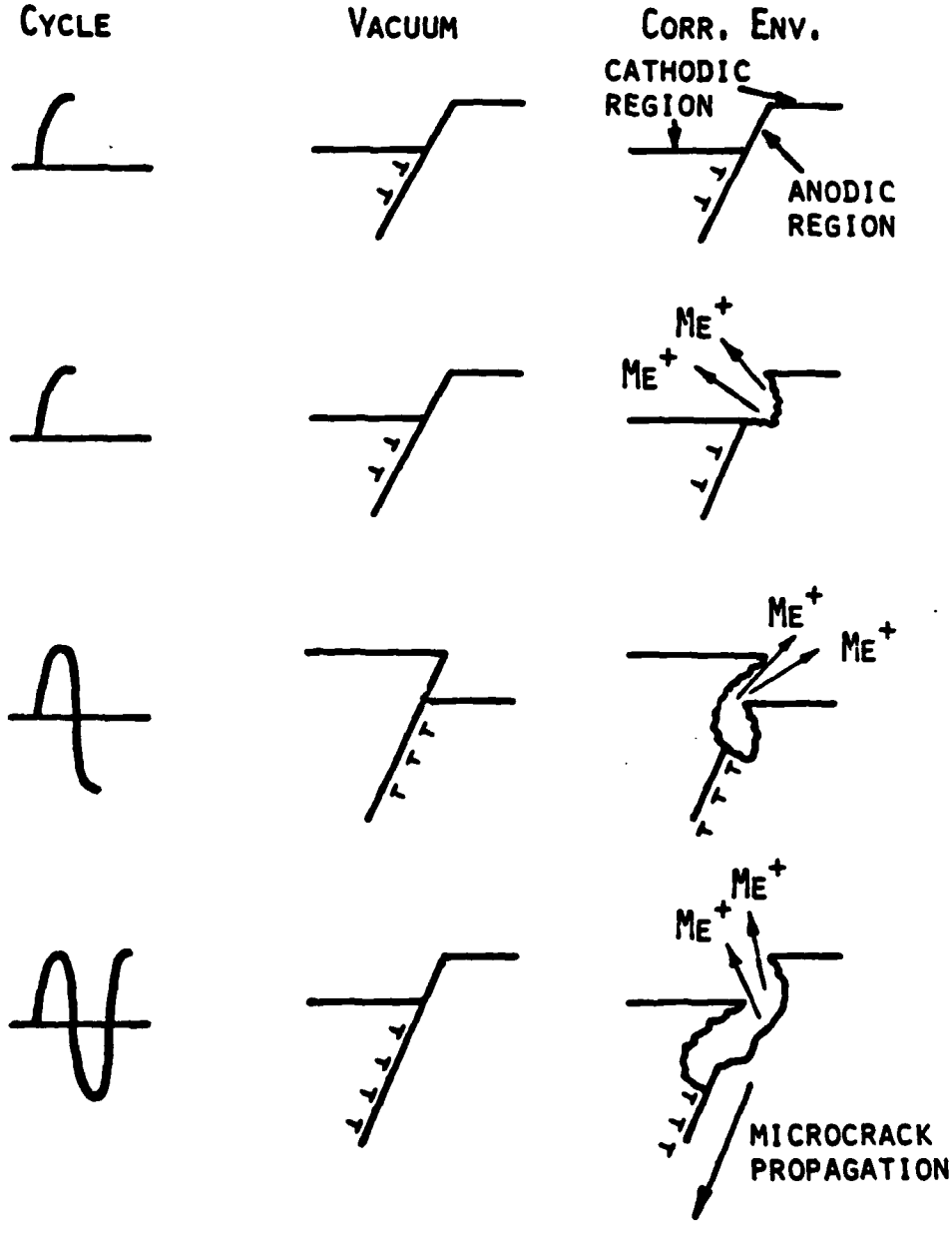

DRIVING FORCE

$\Delta\sigma$ AND ELECTROCHEMICAL POTENTIAL

Figure 1 Phenomenological Representation for Corrosion Fatigue Crack Initiation

3.3 PRELIMINARY MODELING WORK FOR INITIATION METHODOLOGY

Based on the initiation phenomenon described in the previous section, models for quantitatively predicting fatigue crack initiation life in a corrosive environment can be developed. Two mechanistic models can be used; the stress-initiation life model [64,66-68] and the strain-initiation life model [69-71]. These models can be modified for a case of spectrum loading in a corrosive environment either by the RMS method [e.g., 72,73] or the Palmgren-Miner linear cumulative damage rule [74,75].

3.3.1 Stress-Initiation Life Model

For blunt notches including fastener hole type, Kim, Fine, and Mura [66,67] derived the number of cycles to fatigue crack initiation for constant amplitude loading. In their study, elastic-plastic micromechanics at the tip of a smooth ended notch or fastener hole [64,68] was extended to the cyclic loading case in order to predict the number of cycles to crack initiation. The number of cycles to initiation was derived to be a function of effective stress amplitude, $\Delta\sigma_{eff}$; notch geometry (circular for fastener holes), and some measurable material properties such as

cyclic work hardening rate, Young's modulus and cyclic yield stress.

The resulting equation for predicting crack initiation life for a fastener hole is described by Eq. 1.

$$N_i = A\left[E\,(1 + n')\right] \cdot \left[\Delta\sigma_{eff}^2 - \Delta\sigma_{th}^2\right]^{-1} \qquad (1)$$

where each parameter is defined in Fig. 2. Since "A" and the $\Delta\sigma_{th}$ are determined experimentally, Eq. 1 is semi-empirical. Fig. 2 schematically represents the relationships between plots of log N_i vs. log $[\Delta\sigma_{eff}^2 - \Delta\sigma_{th}^2]$ and those of N_i vs. $\Delta\sigma_{eff}$. Eq. 1 predictions fit the well-known S-N type curve used in fatigue analysis. Experimental data for supporting this relationship is compiled in Refs. 64 and 65. The value of "A" in Eq. 1 is expected to be smaller in a corrosive environment due to load-electrochemical interaction. In Eq. 1, since the fatigue crack initiation life decreases as "A" decreases, the "A" value should indicate the severity of the environment.

3.3.2 Strain-Initiation Life Model (Modified Coffin-Manson Approach)

Coffin and Manson [69,70] established that plastic strain-life data could be linearized with log - log

Stress-Initiation Life Model (Critical Local Plastic Strain Accumulation Crit.)

$$N_i = A\left[E \cdot (1 + n')\right]\left[\Delta\sigma_{eff}^2 - \Delta\sigma_{th}^2\right]^{-1}$$

(Kim, Fine & Mura, 1979)

(Ref. 68)

A = Emp. Const.
E = Young's Modulus
n' = Cyclic Work Hardening Exp.
$\Delta\sigma_{eff} = \sigma_{MAX} - \sigma_{MIN}$
$\Delta\sigma_{th}$ = Threshold Value (Experimental Value)
N_i = Cycles To Initiation

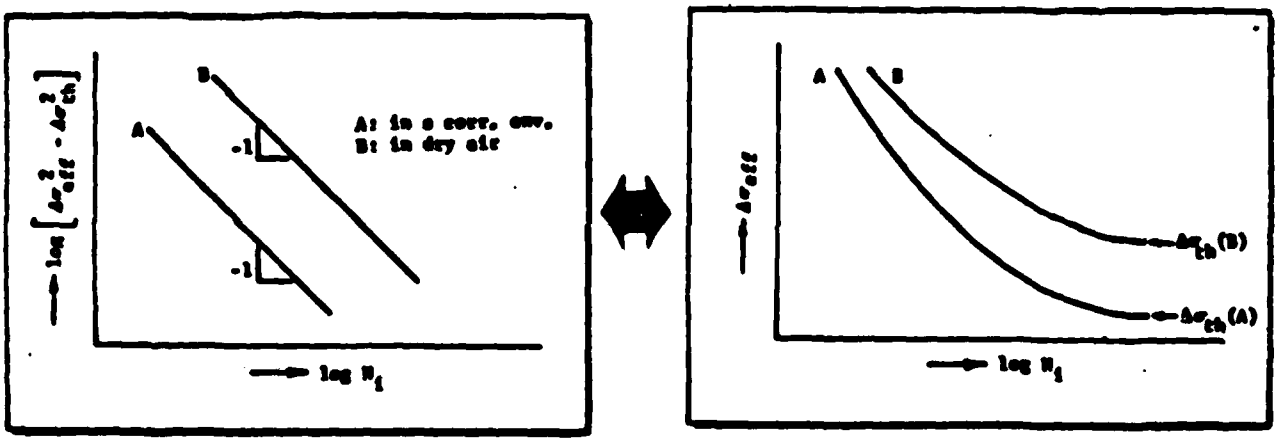

Figure 2 Schematic Representation of Stress-Initiation Life Model

coordinates. Using data for several metals and alloys, plastic strain and cycles to failure have been related by the power-law Eq. 2. Various alloys, including 7075-T7651 aluminum alloy and β-annealed Ti-6Al-4V alloy have been evaluated [71,76].

$$\frac{\Delta \epsilon_p}{2} = \epsilon'_f (2N_f)^c \qquad (2)$$

where $\Delta\epsilon_p/2$ = plastic-strain amplitudes

$2N_f$ = reversals to failure (thus N_f cycles to failure).

c = fatigue-ductility exponent

ϵ'_f = fatigue-ductility coefficient

More recently, increased attention has been given to the suggestion that the Coffin-Manson type of strain-life approach works best for strain-initiation life data [77,78], also verified by many investigators [60,79]. Eq. 2 can be modified for crack initiation applications by substituting N_i for N_f to obtain Eq. 3. In Eq. 3, the parameters c and

ϵ_f' are determined from plots of $\Delta\epsilon_p$ vs. N_i instead of $\Delta\epsilon_p$ vs. N_f plots.

$$\frac{\Delta\epsilon_p}{2} = \epsilon'_f (2N_i)^c \tag{3}$$

Fig. 3 schematically shows how cyclic strain-life parameters can be determined from the plots of log of strain amplitude vs. log of cycles to fatigue crack initiation (modified Coffin-Manson plots). The total applied cyclic strain amplitude is the sum of two components, elastic strain and plastic strain. From Fig. 3, elastic and plastic strain may be expressed by Eq. 5 and Eq. 6, respectively.

Total strain; $$\frac{\Delta\epsilon}{2} = \frac{\Delta\epsilon_e}{2} + \frac{\Delta\epsilon_p}{2} \tag{4}$$

Elastic strain; $$\frac{\Delta\epsilon_e}{2} = \frac{\sigma_f'}{E} \cdot (2N_i)^b \tag{5}$$

Plastic Strain; $$\frac{\Delta\epsilon_p}{2} = \epsilon_f' \cdot (2N_i)^c \tag{6}$$

These parameters may be determined in a modified Coffin-Manson type of N_i vs. $\Delta\epsilon$ graph, as shown in Fig. 3. Total strain can be expressed by these cyclic parameters and N_i, cycles to initiation. Thus,

$$\frac{\Delta\epsilon}{2} = \frac{\sigma_f'}{E} (2N_i)^b + \epsilon_f' (2N_i)^c \tag{7}$$

Strain-Initiation Life Model (Modified Coffin-Manson Type LCF App.)

$$\frac{\Delta\epsilon}{2} = \underbrace{\frac{\sigma_f'}{E}(2N_i)^b}_{\text{Elastic}} + \underbrace{\epsilon_f'(2N_i)^c}_{\text{Plastic}}$$

$\Delta\epsilon$ = Total Strain (Strain-Controlled)
σ_f' = Fatigue-Strength Coeff.
ϵ_f' = Fatigue-Ductility Coeff.
b = Fatigue-Strength Exp.
c = Fatigue-Ductility Exp.
N_i = Cycles To Initiation

$\frac{\Delta\epsilon_p}{2} = \epsilon_f'(2N_i)^c$

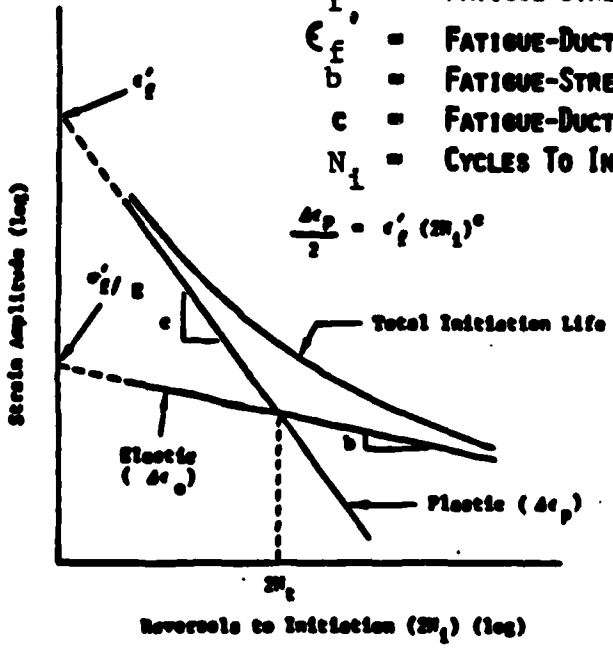

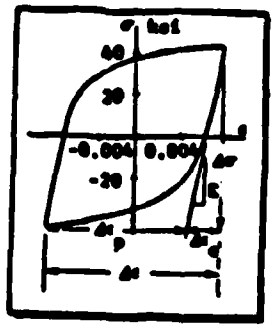

Figure 3 Schematic Representation of Strain-Initiation Life Model

The parameters in Eq. 7 are expected to vary depending on the environment, and they can be determined using strain-initiation life data for a given environment. Then, Eq. 7 can be used to estimate the initiation life. This method is promising for estimating the corrosion fatigue crack initiation life of mechanically-fastened joints. The fatigue crack initiation life is expected to be a major portion ($\simeq$ 50%-90%) of the total fatigue life.

3.3.3 Application of Initiation Models for Spectrum Loading

The stress-initiation life model and the strain-initiation life model must be modified for spectrum loading applications. Two potential methods for handling spectrum loading are discussed in this section.

3.3.3.1 Root Mean Square Approach

The root mean square (r.m.s.) approach has been used by Press et al [80] to evaluate load spectra. This approach has also been used to simulate the random load history for structural joint [81] and to predict the fatigue crack propagation in steel under spectrum loading [72]. The basic objective of the r.m.s. approach is to represent the

spectrum loading with an equivalent constant amplitude loading that will have the same effect on the fatigue behavior as the spectrum loading.

The key parameter in the stress-initiation life model and the strain-initiation life model is delta stress ($\Delta\sigma$) and delta strain ($\Delta\epsilon$), respectively. These parameters can be expressed in an r.m.s. form [73] as follows.

$$\Delta\sigma_{rms} = \sqrt{\frac{\sum_{i=1}^{k} \Delta\sigma_i^2}{n}} \tag{8}$$

$$\Delta\epsilon_{rms} = \sqrt{\frac{\sum_{i=1}^{k} \Delta\epsilon_i^2}{n}} \tag{9}$$

It may be possible to use the r.m.s. approach for crack initiation application if suitable methods are developed to account for load interaction effects on the plastic zone size.

3.3.3.2 Cumulative Damage Approach

Another technique used to ascertain structural life or initiation life under spectrum loading and in a corrosive environment is the cumulative-damage criterion. The

simplest failure criterion is the Palmgren-Miner Linear-Cumulative Damage rule, which has long been used by designers in the aerospace industry. Initiation life in a corrosive environment can be determined with the stress-initiation life model as shown in Fig. 4 or with the strain-initiation life model in a similar manner. Since this kind of curve is obtained from constant amplitude tests, load spectra must be simplified to utilize the Palmgren-Miner rule. For spectrum loading the loads may be distributed throughout the spectrum in a random manner, but the resulting spectrum is fixed and thus deterministic. Load spectra can be simulated in a much simpler format using various methods [74,75]. Once the number of cycles at a given stress level is determined, the Palmgren-Miner damage rule can be used to predict corrosion fatigue crack initiation life from stress-initiation life or strain-initiation life data. The Palmgren-Miner rule is mathematically expressed in Eq. 10.

$$d = \frac{n_i}{N_i} \qquad \text{at a given stress level, } \sigma_i. \tag{10}$$

where d = damage at σ_i

n_i = number of cycles at σ_i

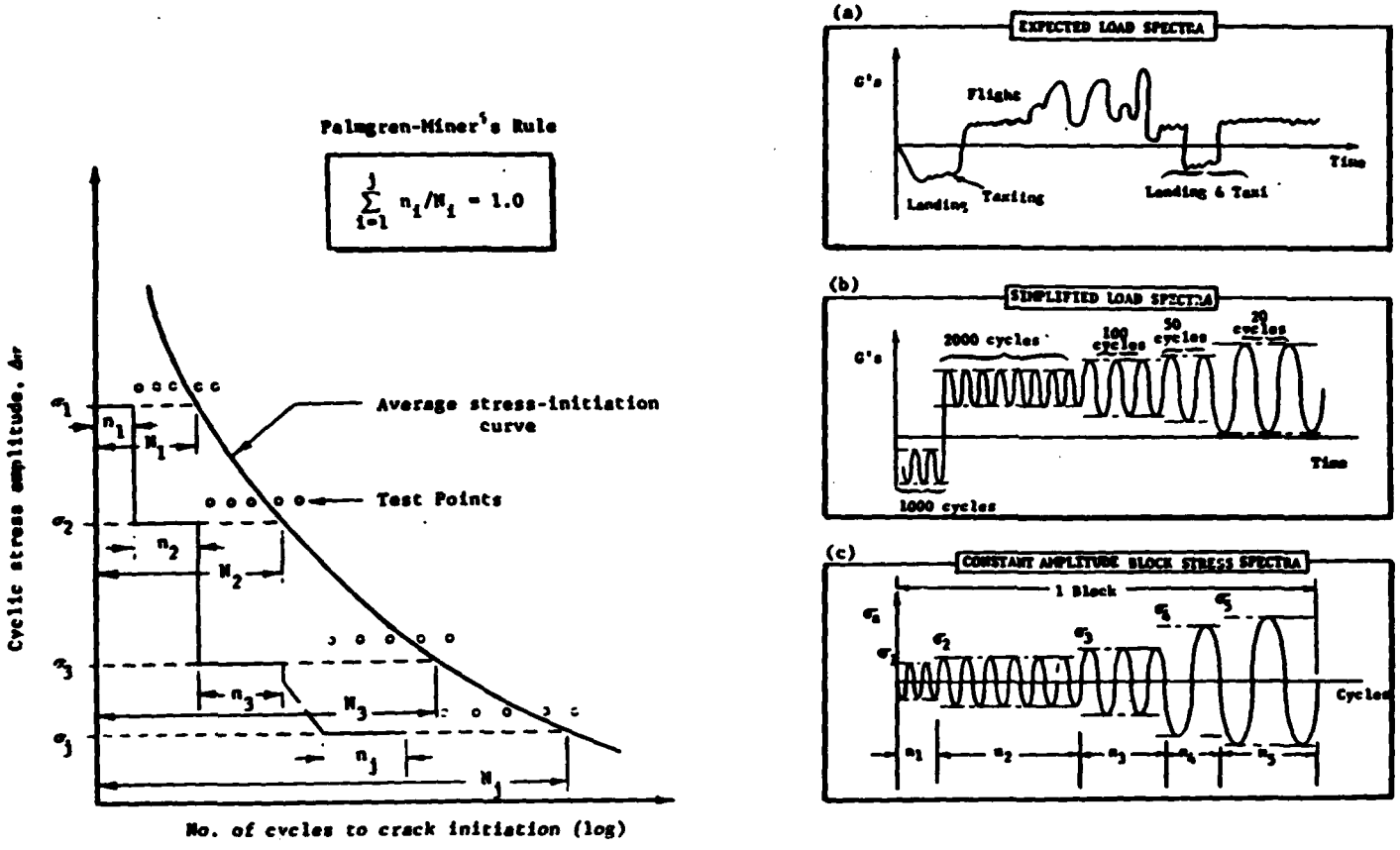

Figure 4 Example of Application of the Initiation Model to Spectrum Loading

N_i = number of cycles to fatigue crack initiation at σ_i and accordingly, fatigue crack initiation occurs when

$$\sum_{i=1}^{j} \frac{n_i}{N_i} = \left(\frac{n_1}{N_1} + \frac{n2}{N2} + \frac{n3}{N3} + \cdots + \frac{n_j}{N_j}\right) = 1 \qquad (11)$$

Following the above procedure, the time-to-crack-initiation for a given load spectrum can be estimated. The following information is needed to use this method.

- o The number of cycles spent at each given stress level for a given time
- o Stress concentration factor for a fastener hole or a fastened joint
- o Stress-initiation life data or strain-initiation life data over the applicable stress (or strain) amplitude range and in the selected environment.

The method described above is useful not only for predicting fatigue crack initiation life but also for overall life by simply using a σ-N_f type of curve, rather than σ-N_i as in Fig. 4.

THIS PAGE INTENTIONALLY LEFT BLANK

SECTION IV

CORROSION FATIGUE CRACK PROPAGATION

4.1 INTRODUCTION

The purpose of this section is to discuss the corrosion fatigue (CF) crack propagation problem and to review current state-of-the-art tools for addressing this problem. Specifically, the following will be included in this section: (1) historical background review, (2) CF state-of-the-art review, (3) critical review of existing models, (4) effect of corrosive environment on crack retardation, and (5) load interaction models for spectrum loading.

4.2 HISTORICAL BACKGROUND

With the development of fracture mechanics technology, increased emphasis has been placed on fatigue crack growth in many applications since the early 1950s. Since fatigue damage in most applications was known to result from the conjoint actions of the cyclically applied stress and external environment, corrosion fatigue crack growth study became essential to assure structural integrity, durability, and reliability, together with optimum structural

efficiency. Thus, studies of the influence of environments on fatigue crack growth began in the mid-1960s and have continued throughout the past 15-20 years. The results from the various studies have been reviewed and summarized in a number of papers [82-90], proceedings of conferences [91-98], and in books [73,99-100].

As a phenomenological understanding was in progress, a number of important issues that provided a rational basis for predicting environment-assisted fatigue crack growth began to crystallize by the early 1970s. These issues relate to the reported differences in response to frequency and waveform for aluminum alloys [101-107] and for steels [108-114], the relationship between environment-assisted sustained-load crack growth (stress corrosion cracking) and corrosion fatigue crack growth [85,115,116], and the cause or mechanism for environment-assisted crack growth below the so-called stress corrosion cracking threshold, K_{Iscc} [117,118].

4.3 STATE-OF-THE-ART REVIEW

In the late 1960s, Bradshaw and Wheeler [101,105,107] showed that the rate of fatigue crack growth at a given stress intensity level, K, appeared to depend on the product

of water vapor pressure and cyclic load period (1/frequency), and suggested that the observed frequency effect resulted from the time available for the reaction of water vapor with the newly created crack surfaces. In distilled water, on the other hand, aluminum alloys were reported to exhibit little or no effect of frequency [104,119]. Based on the assumption of no synergistic interaction between fatigue loadings and environment, Wei and Landes [120] hypothesized a linear summation model to predict the corrosion-fatigue behavior above K_{Iscc} for a high-strength steel. The model considers the corrosion fatigue crack growth rate above K_{Iscc} to be the sum of the rate of fatigue crack growth in an inert reference environment and an environmental component that is computed from the load profile and sustained-load crack growth data obtained in an identical aggressive environment. Wei and Landes [120] could satisfactorily predict the rates of corrosion-fatigue-crack growth for 18-Ni Maraging steels tested in several gaseous and aqueous environments based on this model.

However, even at K levels below K_{Iscc}, where the sustained-load crack growth is not expected to contribute primarily to corrosion fatigue crack growth, significant effects of frequency on crack growth rate have been observed

and reported for high-strength steels [108,110,112]. The effects of frequency on crack propagation for aluminum alloys has also been investigated for constant amplitude loading [104,119]. Most researchers agree that there must be a synergistic interaction between environment and fatigue loading and that this interaction may be the key factor for contributing to crack growth enhancement below K_{Iscc} level. Accordingly, Wei and Landes' linear summation model is believed to have only limited applicability for environment-material systems in which the material is highly susceptible to the environment. Such examples include high-strength steels having yield strength greater than approximately 200 ksi tested in distilled water or 3.5% NaCl.

Recent NADC and AFFDL programs [121-123] performed by Saff et al. have developed a semi-empirical method for quantitatively predicting crack growth behavior in synthetic sea water by applying the Wei-Landes' linear superposition approach to several landing gear steels subjected to various load spectra. In view of a high susceptibility of landing gear steels (such as 300M steel) to an environment, this method was successfully used for propagation life prediction. However, this method does not directly apply to all airframe structural materials, most of which are not susceptible to the environment, since the method does not

account for the synergistic interaction between fatigue loading and environment for these alloys.

Based on the recently developed understanding and on research over the past 15 years, a rational basis for treating environment-assisted fatigue crack growth has been suggested [124]. The rate of fatigue crack growth in an aggressive environment, (da/dN), is considered to be the sum of three components:

$$(da/dN)_e = (da/dN)_i + (da/dN)_c + (da/dN)_{scc}.$$

$(da/dN)_i$ is the rate of fatigue crack growth in an inert environment, and represents the contribution of "pure" (mechanical) fatigue. This component is essentially independent of frequency at temperature where creep is not important. $(da/dN)_c$ represents a cycle--dependent contribution requiring synergistic interaction of fatigue and environmental attack. $(da/dN)_{scc}$ is the contribution by sustained-load crack growth (i.e., by stress corrosion cracking) at K levels above K_{Iscc}, and would be a function of sustained-load frequency, load ratio and waveform. Existing models for the second term, $(da/dN)_c$, considered to be the dominating factor for crack growth below K_{Iscc}

level, are reviewed in subsection 4. The third term in Eq. 12, $(da/dN)_{scc}$, follows directly from that for sustained-load crack growth, which has been well described by Wei [125].

Since 1977, when synergistic interaction was identified to be the major contribution in most applications and a quantitative basis for treating corrosion fatigue crack growth was established, phenomenological understanding has significantly progressed. Through the integrated interdisciplinary studies [126] and comparisons of activation energies for crack growth and for surface reaction [127,128], the rate-controlling process for crack growth for a high-strength steel (AISI 4340) was identified to be a slow step in the reaction of water/water vapor with iron and, perhaps, iron carbide [126,127]. This reaction step is associated with the nucleation and growth of oxide on the surface, and the presumed accompanying production of hydrogen [126]. Hydrogen produced by this reaction is believed to be responsible for embrittlement.

Having identified the rate-controlling process for sustained-load crack growth for this high-strength steel in water/water vapor, Pao, Wei, and Wei [129] examined its implication in terms of environment-assisted fatigue crack

growth response. Their results indicated that both steady-state and non-steady-state crack growth response can be adequately explained in relation to the kinetics of surface reactions. Based on this success, the integrated interdisciplinary approach has been extended to the study of environment-assisted fatigue crack growth response in an aluminum alloy [130]. This later study expands on an earlier suggestion by Bradshaw and Wheeler [101,107] that the enhancement of fatigue crack growth in aluminum alloys by water vapor is determined by the exposure (pressure x time) during each load cycle. It has led to the recognition that for highly reactive systems, environment-assisted crack growth may be controlled by the transport of the aggressive environment to the crack tip. This observation has led to the development of transport and surface reaction-controlled models for environment-assisted fatigue crack growth. Additional verification of the transport-controlled model has been made also for a hydrogen sulfide-steel system [131].

Two separate regimes have now been identified, in which environment enhancement of fatigue crack growth is determined by the occurrence of surface reaction during one loading cycle. For alloy-environment systems with "slow" reaction kinetics (e.g., steel-water vapor system),

environmental effects are evident at "high" pressures and "low" frequencies, and crack growth enhancement is only a function of the surface reaction kinetics. On the other hand, for alloy-environment systems with "fast" reaction kinetics (e.g., aluminum-water vapor and steel hydrogen sulfide systems), environmental effects now manifest themselves at "low" pressures and "high" frequencies, and the enhancement of crack growth now also depends on the rate of transport of the external environment to the crack tip. The eight (8) orders of magnitude difference between the rates of water vapor reactions with aluminum alloys and with steels [126,129,130], and of water vapor and hydrogen sulfide reactions with steel [131] can readily account for the observed differences in environment-assisted fatigue crack growth response for these alloys and environment.

Meanwhile, understanding of fatigue crack growth behavior in aqueous environments is much less advanced. It appears that almost the same concept of sequential processes is involved in embrittlement by external environments. The only essential problem involves identification of the rate-controlling process. In other words, it is very important to determine the slowest process in the alloy-environment systems to be investigated in this program, because this process will directly affect the life prediction method. A

diffusion-controlled model has been developed based on the assumption that there is an ample supply of hydrogen atoms at a crack tip [132]. Details of this model are given in Volume I of this report. Since the extent of reactions of water vapor with aluminum and titanium alloys is limited, the assumptions used for the diffusion-controlled model for an aqueous environment must be carefully examined with the experimental data provided in Phase I.

To obtain reliable service life predictions environmentally-induced effects must be properly accounted for. The existence of a cycle-dependent term and its frequency dependence has not been fully appreciated by most of the engineering community. This incomplete appreciation is reflected in the "indiscriminate" use of "accelerated" tests and in disregarding cyclic load frequency as a significant design variable. The impact of this cycle-dependent term must be recognized and taken into proper account in the development of realistic design data and in propagation life estimation. The models developed on the basis of current understanding of environment-assisted fatigue crack growth provide a useful starting point for the development of more meaningful and reliable testing and design procedures.

4.4 A CRITICAL REVIEW OF EXISTING MODELS

In this section, the current models for the cycle-dependent component of environmentally-assisted fatigue crack growth are reviewed. Included in the discussion are a transport-controlled model [133,134], a surface-reaction-controlled model [133,125], and a diffusion-controlled model [132].

Recent fracture mechanics and surface chemistry studies of sustained-load and fatigue crack growth in high-strength alloys exposed to gaseous environments suggest hydrogen embrittlement as the mechanism responsible for the enhancement of crack growth. The overall crack growth response, however, is governed by one or more of a number of sequential processes that culminate in embrittlement by hydrogen. As shown in Fig. 5, these processes include:

1. Transport of the gas or gases to the crack tip.

2. Sequential processes involved as the gas or gases react with newly created crack surfaces to evolve hydrogen (such as physical and dissociative chemical abosrption).

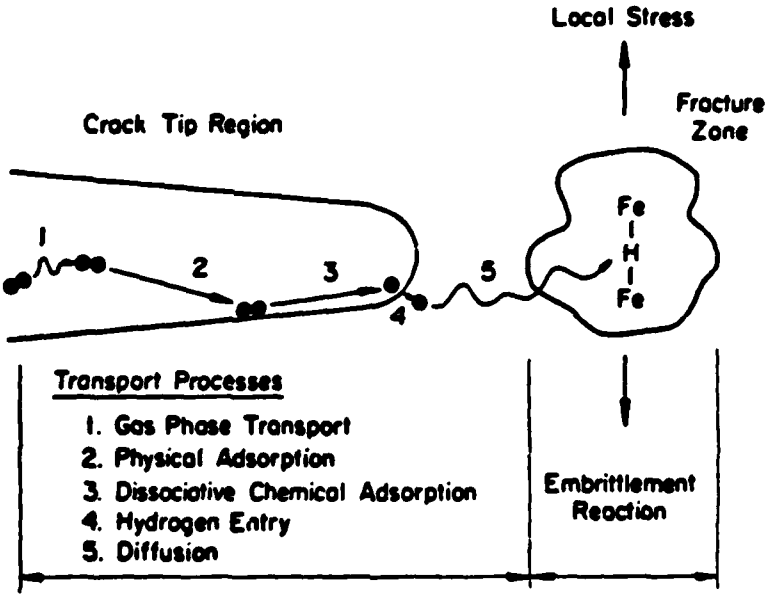

Figure 5 Schematic Representation of Rate Processes for Corrosion Fatigue in a Gaseous Environment

3. Hydrogen entry (or absorption).

4. Diffusion of hydrogen to the fracture (or embrittlement) site.

5. Hydrogen-metal interaction leading to embrittlement of enhancement of crack growth (i.e., the embrittlement reaction).

It appears that the rate control concept can be extended to the considerations of crack growth response in aqueous environments. The first step in the sequence described above is replaced by liquid transport or by the transport of specific species in solution, and the second step by liquid-solid reactions described by Eq. 13 for aluminum alloys in a water environment:

$$\left.\begin{aligned} &Al \longrightarrow Al^{3+} + 3e^- \\ &2\,Al^{3+} + 3H_2O \longrightarrow Al_2O_3 + 6H^+ \\ &6H^+ + 6e^- \longrightarrow 6[H] \end{aligned}\right\} \qquad (13)$$

A phenomenological understanding for the diffusion-controlled process is shown schematically in Fig. 6.

MECHANISM FOR 2ND TERM, $(da/dN)_c$

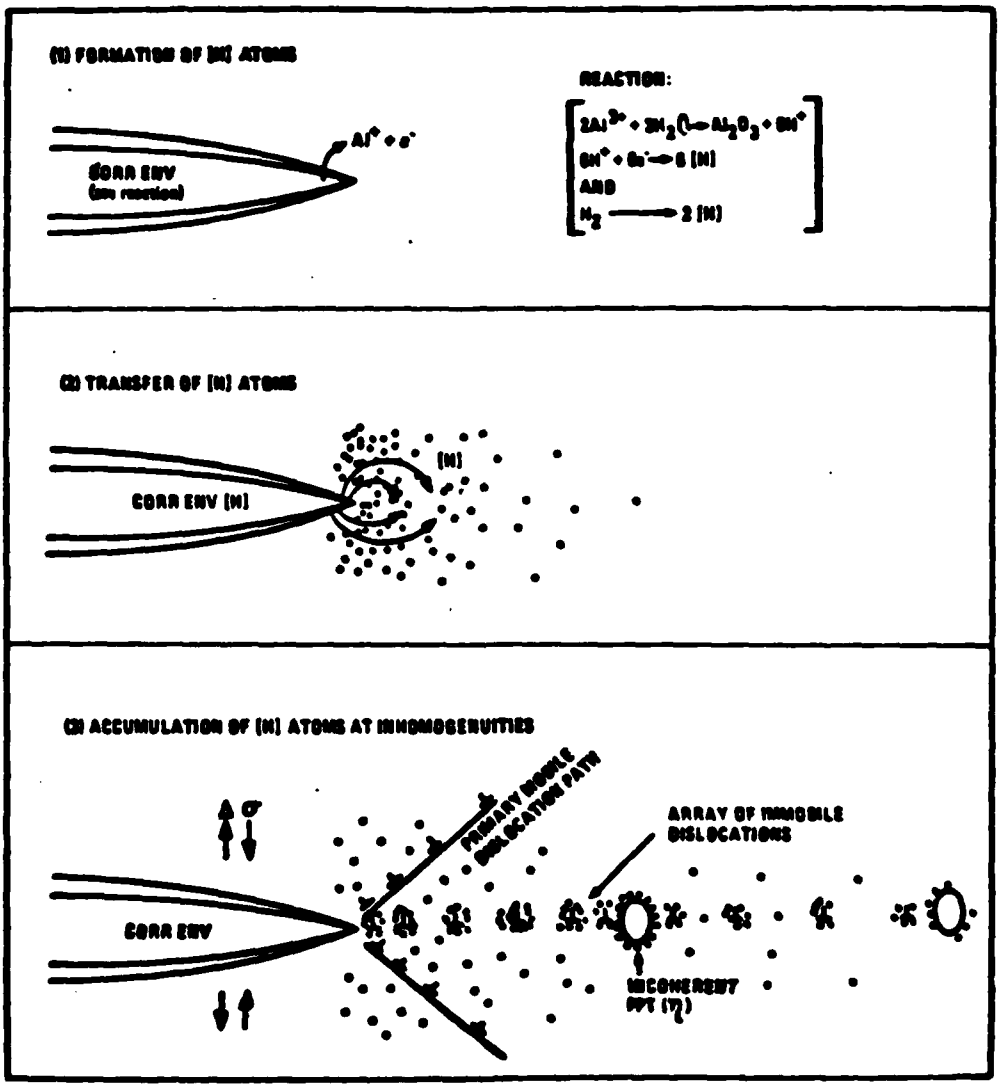

Figure 6 Schematic Representation of Diffusion-Controlled Rate Process for Corrosion Fatigue in a Aqueous Environment

Modeling for environmentally-assisted crack growth has been made according to the sequence described above. For fatigue loading case, models have been proposed by Lehigh Univ. (LU) investigators for transport and surface-reaction controlled crack growth. The models are based on the three-term superposition concept described by Eq. 12. The specific models for $(da/dN)_c$ are as follows:

Transport Control:

$$(p_o/2f)_s = \left[436\ \frac{\beta^*}{\alpha} f(R)\ \frac{\sigma_{ys}^2}{N_o kTE^2}\left(\frac{T}{M}\right)^{1/2}\right]^{-1} \tag{14}$$

$$\frac{(da/dN)_c}{(da/dN)_{e,s}} = 436\ \frac{\beta^*}{\alpha} f(R)\ \frac{\sigma_{ys}^2}{N_o kTE^2}\left(\frac{T}{M}\right)^{1/2}\ \frac{p_o}{2f} \tag{15}$$

$$\frac{(da/dN)_c}{(da/dN)_{c,s}} = \frac{(p_o/2f)}{(p_o/2f)_s} \tag{16}$$

$$f(R) = \frac{1}{4}\left[\left[\frac{1+R}{1-R}\right]^2 + \frac{1}{2}\right] \tag{17}$$

Surface Reaction Control:

$$\frac{(da/dN)_c}{(da/dN)_{e,s}} = 1 - \exp(-k_c p_o/2f) \tag{18}$$

$$\frac{(da/dN)_c}{(da/dN)_{c,s}} = 1 - \exp(-k_c p_o/2f) \tag{19}$$

Diffusion Control:

$$\left[\frac{da}{dN}\right]_c = A \exp(-G_B/RT)\ \sqrt{pDt}\ (\Delta K/\sigma_o')^2;\ t = 1/2f \tag{20}$$

In the transport and surface reaction controlled models, subscript s denotes the values at saturation, which is defined as the maximum in environmental effect and corresponds to the attainment of complete reactions with the active crack surfaces during each loading cycle. The terms in Eqs. 14-20 are as follows: f = cyclic load frequency; k_c = reaction rate constant; M = molecular weight of the gas; N_o = density of surface sites; P_o = pressure of gas in the surrounding environment; k = Boltzmann's constant; and T = absolute temperature. E and σ_{ys} are the elastic modulus and yield strength of the material, respectively. The parameter β^*/α is a ratio of empirical constants for surface roughness and flow, and appears to be a constant (equal to approximately 3.8). For the diffusion-controlled model, A = proportionality constant; G_B = binding energy of hydrogen atoms to a dislocation; R = gas constant; p = pressure; D = diffusivity of hydrogen; t = time available for reaction; and σ'_o = cyclic yield stress. For consistency, t is again taken to be equal to 1/2f.

For design applications, it is necessary to assess the validity and to define the range of applicability of each model. A considerable amount of experimental support has been developed at LU for the transport-controlled model. Some support for the other two models is available; however,

they must be supplemented by additional data from this program and others. The range of applicability of the models is governed by the transfer of control from one rate-controlling process to another. The environmental conditions (such as pressure and temperature) that dictate this transfer of control may be determined, in principle, by equating $(da/dN)_c$ for each case and then calculating the pressure-temperature relationship for the transfer. For example, the transfer between transport and diffusion control is given Eq. 21,

$$P_o = (C_d/C_t)^2 \, T \exp \left[- (2G_B + E_d)/RT \right] \qquad (21)$$

where E_d is the activation energy for hydrogen diffusion, and C_d and C_t contains terms in the model that do not involve environmental parameters. In practice, prediction of the conditions for transfer can be made only if the parameters in the models are known to be sufficiently accurate and detailed. Some specific comments can be made, however, with respect to the aluminum and titanium alloys and environments that are of interest to this program.

Measurements of the kinetics of reactions of water vapor with aluminum and titanium alloys have been made at LU under previous programs. These measurements indicate that these

reactions are extremely rapid (corresponding to an initial sticking coefficient of nearly 1). As such, the surface reaction cannot be the rate-controlling process for these alloy-environment systems. For gases, therefore, fatigue crack growth conforms to transport control at $(P_o/2f)$ below the saturation, $(P_o/2f)s$. Typically, $(P_o/2f)s$ is of the order of 10 pa-s. At $(P_o/2f$ greater than $(P_o/2f)s$ and in aqueous environments, one would expect transfer of control to one of the subsequent processes; possibly hydrogen diffusion. In aqueous salt water environments, this transfer is suggested by GD/FWD data [132] on a 7075-T6 aluminum alloy as well as others [135,136].

However, the essential problem involves the model assumption. The model was derived on the basis of considerations of rate-controlling processes, and do not allow for other restrictions. The diffusion-controlled model was derived, therefore, with the implicit assumption of ample supply of hydrogen at a crack tip. At the present time, it is not clear whether the assumption of continuous supply of hydrogen is valid for the case of aqueous environments, or whether liquid-phase transport might be rate-controlling. In any case, the pressure term in the model may have to be replaced or redefined, perhaps by

hydrogen fugacity at the input surface. Further work is required to resolve these critical issues.

4.5 THE EFFECT OF CORROSIVE ENVIRONMENT ON CRACK RETARDATION

The effect of corrosive environment on crack retardation in various materials due to a single overload has been reported [137-140]. The highlights of the experimental findings for retardation in a corrosive environment for aluminum alloys are as follows:

1. Retardation due to the overload was observed to occur in air as well as in a more corrosive environment such as 3.5% NaCl solution.

2. In both non-aggressive and aggressive environments, the amount of retardation (i.e., the number of delay cycles) was found to be mainly a function of three factors: Material/microstructure, stress intensity range (ΔK) and overload ratio. The number of delay cycles is greater with higher overload ratio or lower ΔK.

3. The amount of retardation was less in a corrosive environment than in dry air for the same ΔK and overload ratio. This is attributed to the fact that in the corrosive

environment fewer cycles are required for fatigue cracks to propagate through the plastic zone created by the previous overload, since the crack growth rate is higher in the corrosive environment.

As explained above, the differences in the amount of retardation in dry air and in a corrosive environment appear to be caused simply by a faster crack growth in a corrosive environment than in dry air. Therefore, these retardation effects will be readily accounted for in the parameters of the crack growth enhancement term in the superposition scheme.

From this point of view, it is believed that modeling for retardation in a corrosive environment can be accomplished easily, once the rate-controlling process is identified for aluminum (or titanium) - aqueous environment system. Apparently, no well-established method to predict crack retardation in a corrosive environment exists at this time.

4.6 LOAD INTERACTION MODELS FOR SPECTRUM LOADING

This sub-section describes various existing models for spectrum loading to properly account for load-interaction or

retardation. Each parameter is defined in Fig. 7. Since details of each model are well described in Refs. [141-146], only the resulting equations will be described and discussed.

4.6.1 Generalized Wheeler Model

$$a_N = a_o + \sum_{i=1}^{N} C_i \cdot f(\Delta K, R) \tag{22}$$

$$\text{If } K_{max}^{i} \geq K_{max}^{*};\ C_i = 1 \text{ (no retardation)} \qquad K_{max}^{i} < K_{max}^{*};\ C_i = \left(\frac{K_{max}^{i}}{K_{max}^{*}}\right)^{2m} \tag{23}$$

$$K_{max}^{*} = K_{max}^{OL}\left(1 - \frac{\Delta a_i}{Z_{OL}}\right)^{1/2} \tag{24}$$

K_{max}^{*} is the value of maximum stress intensity factor to create a plastic zone size equal to Z_i, and can be calculated by Eq. 24 using the input information of K_{max}^{OL}, Δa_i, and Z_{OL}, which can be obtained either from the

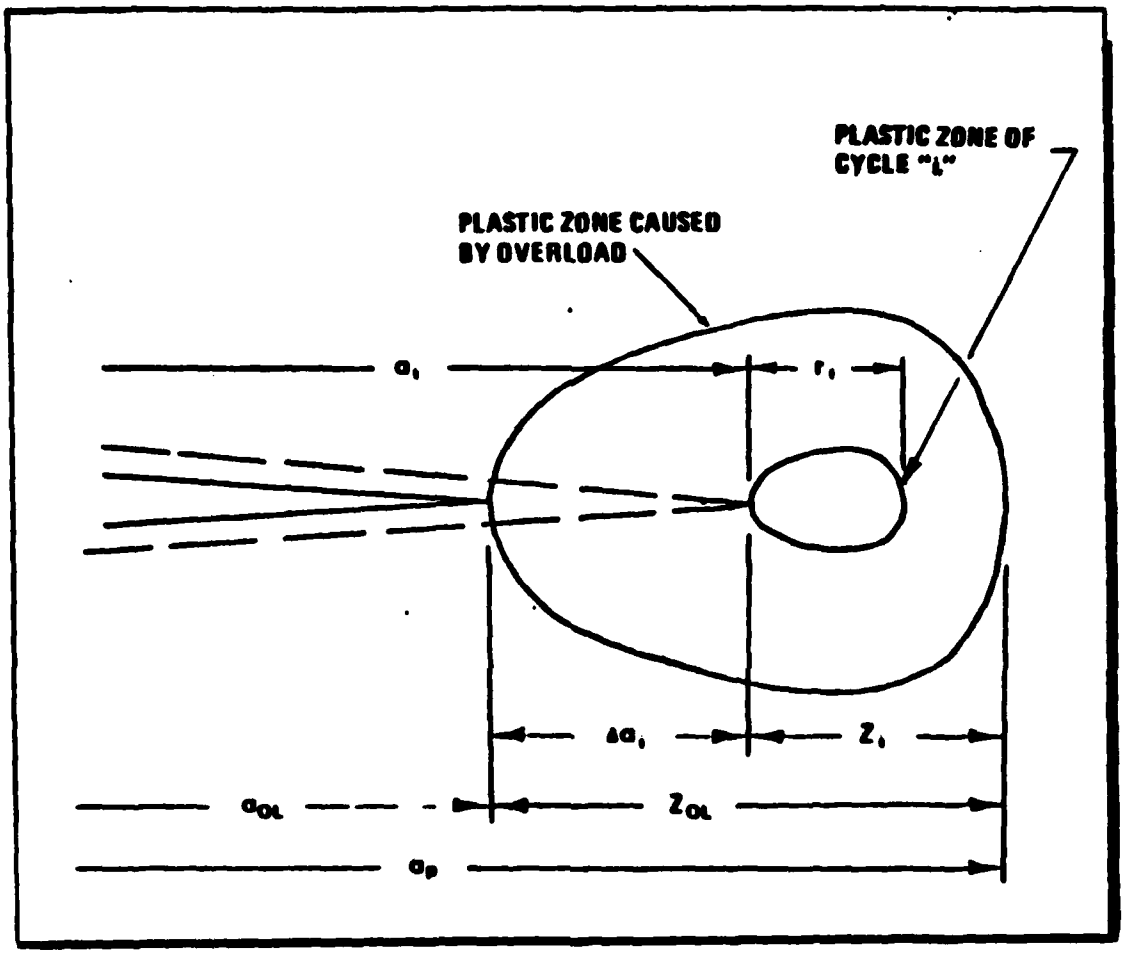

Figure 7 Plastic Zone Sizes and Notation Used for Load Interaction Models

calculation for the previous cycle or from the computer memory. Wheeler's retardation factor, C_i, can then be obtained by Eq. 23 . This reduction factor, C_i, will adjust the incremental crack growth for each cycle, as shown in Eq. 22. If Paris' equation for f(ΔK,R) is used, ΔK_{eff} will be simply $(K^i_{max} / K^*_{max})^{2m/n} \cdot \Delta K$.

4.6.2 Generalized Willenborg Model

$$a_N = a_o + \sum_{i=1}^{N} f(\Delta K_{eff}, R_{eff}) \tag{25}$$

$$(K^i_{max})_{eff} = K^i_{max} - \Phi \left[K^i_{red}\right] \tag{26}$$

$$(K^i_{min})_{eff} = K^i_{min} - \Phi \left[K^i_{red}\right] \tag{27}$$

$$K^i_{red} = K^{oL}_{max} \left(1 - \frac{\Delta a_i}{Z_{oL}}\right)^{1/2} - K^i_{max} \tag{28}$$

$$\Phi = \left[K^i_{max} - (K_{max})_{TH}\right] \Big/ \left[K^{oL}_{max} - K^i_{max}\right] \tag{29}$$

$$\Delta K_{eff} = K^i_{max} - \Phi \left[K^i_{red}\right] - \left\{K^i_{min} - \Phi \left[K^i_{red}\right]\right\} = \Delta K \tag{30}$$

$$R_{eff} = \frac{K^i_{max} - K^i_{red}}{K^i_{min} - K^i_{red}} \tag{31}$$

In the Willenborg model, as generalized by Gallagher and Hughes [144], the effective stress intensity was considered to be the applied stress intensity minus the reduced stress intensity, K^i_{red}. K^i_{red} is an additional stress intensity required to extend the current interaction zone to that created by the overload, and can be calculated by Eq. 28 . Φ is determined from the shut-off overload experiment for the threshold condition (for $(K^i_{max})_{eff} = (K_{max})_{th}$ $\Delta a = 0$). It is important to note that ΔK_{eff} is identical to ΔK, as shown in Eq. 30 , while only R_{eff} ratio will be changed using the effective maximum (minimum) stress intensity concept, as shown in Eq. 31 . Therefore, this model will primarily depend on the crack growth function, f(ΔK,R), in Eq. 25 . The available equations for F(ΔK,R) are listed in Refs. 146-148.

4.6.3 Generalized Closure Model

$$a_N = a_o + \sum_{i=1}^{N} f(K_{max}, K_{cl}) \tag{32}$$

$$f(K_{max}, K_{cl}) = C \left[\frac{K_{max} - K_{cl}}{1 - C_{fo}} \right]^n \tag{33}$$

$$K_{cl} = \sigma_c \cdot \beta \cdot \sqrt{\pi a} \tag{34}$$

$$C_{fo} = \sigma_c / \sigma_{max} \tag{35}$$

In the above, K_{cl} is the closure stress intensity, σ_c the closure stress, C_{fo} the closure factor, and C and n the

crack growth rate constants, which can be determined from the experiment [145].

4.6.4 Vroman/Chang Model

$$a_N = a_o + \sum_{i=1}^{N} f(\Delta K_{eff}, R) \tag{36}$$

$$f(\Delta K_{eff}, R) = \begin{cases} C \left[\dfrac{\Delta K_{eff}^{i}}{(1-R)^{1-m}} \right]^{n}, & \text{if } R \geq o \\ C \left[(1-R)^{q} \cdot K_{max}^{i} \right]^{n}, & \text{if } R < o \end{cases} \tag{37}$$

$$\Delta K_{eff}^{i} = (K_{max}^{i} - K_{min}^{i}) - A\left[K_{red}^{i}\right] \tag{38}$$

$$K_{red}^{i} = K_{max}^{oL} \left(1 - \frac{\Delta a_i}{Z_{oL}}\right)^{1/2} - K_{max}^{i} \tag{39}$$

where m is Walker's stress ratio correction exponent for $R > o$ and q is Chang's acceleration exponent for $R<o$.

Vroman/Chang's model is essentially a modification of the generalized Willenborg model, using a Walker's crack growth equation for $R > 0$, and Chang's equation for $R < 0$. However, there is a significant difference between these two models. In the Willenborg model, $\Delta K_{eff} = \Delta K$ and R_{eff} is

reduced for the overload (see Eqs. 31 and 28). Therefore, only the effect of the reduced R ratio on crack growth rate contributes to the prediction of retarded crack growth. On the other hand, for the Vroman/Chang model, R ratio is kept constant, while $\Delta K_{eff} = \Delta K - K_{red}$, as shown in Eqs. 38 & 39; therefore, reduction in ΔK_{eff} results in retardation.

Since the amount of reduction in crack growth caused by overload retardation was reported to be significantly greater than that due to a decrease of R ratio, Vroman/Chang's model appears to be more effective in predicting crack retardation behavior for spectrum loading. However, this method still needs to be carefully evaluated using applicable experimental results.

THIS PAGE INTENTIONALLY LEFT BLANK

SECTION V

CONCLUSIONS

The following conclusions are based on this investigation:

1. The intent of the current Navy specifications for achieving corrosion fatigue resistant aircraft structures is quite clear. However, suitable analytical tools, methodology and design data are currently inadequate to demonstrate design compliance and to confidently predict the performance of aircraft structure in service.

2. The corrosion fatigue analysis methodology to be developed should include analytical tools for predicting corrosion fatigue crack initiation as well as crack propagation.

3. Corrosion fatigue analysis methods for predicting crack initiation should be developed based on the interaction of two driving forces: cyclic mechanical force and electrochemical potential.

4. Several variables affect corrosion fatigue behavior. However, the following variables are considered to be the most important for developing the corrosion fatigue analysis methodology under this program: environment, stress level, load spectrum, loading frequency, R-ratio, and holding time. The effect and significances of preconditioning specimens (e.g., pretest and presoak in 3.5% NaCl) on crack initiation and crack propagation should also be investigated.

5. Both the stress-initiation life model [66,67] and the strain-initiation life model [69,70] look promising for predicting the time-to-crack-initiation in a corrosive environment. Further work is required to demonstrate the models for a mechanically-fastened joint subjected to spectrum loading and a corrosive environment.

6. The rate of fatigue crack propagation in a corrosive environment can be considered as the sum of three components: the rate of fatigue crack propagation in an inert environment, a cycle-dependent contribution requiring synergistic interaction of mechanical fatigue and environmental attack, and a contribution due to sustained load crack propagation.

7. Hydrogen embrittlement is the primary cause of corrosion fatigue propagation enhancement. The cycle-dependent component is considered to be the most significant term in the superposition model for corrosion fatigue crack enhancement below K_{Iscc}. The following mechanistic-based models are promising for predicting the cycle-dependent component of fatigue crack propagation: transport-controlled model, surface-reaction-controlled model and diffusion controlled model. These models need to be further evaluated using the experimental data to be acquired under this program.

8. The corrosion fatigue behavior of titanium alloy is very complex. Therefore, it may be difficult to develop a reliable corrosion fatigue analysis methodology for titanium until basic corrosion fatigue mechanisms are better understood.

9. Several retardation models are available for accounting for load interaction effects due to spectrum loading on crack growth. This includes the following models: Wheeler [141], generalized Willenborg [142-144], generalized Closure [145] and Vroman/Chang [146]. These models need to be further evaluated using the experimental data to be acquired under this program.

THIS PAGE INTENTIONALLY LEFT BLANK

REFERENCES

1. SD-24K Volume 1, "General Specification For Design and Construction of Aircraft Weapon Systems"; Vol. 1 - Fixed Wing Aircraft, 13 June 1973.

2. MIL-A-8860(ASG), "Airplane Strength and Rigidity - General Specification For," 18 May 1960.

3. MIL-A-8861(ASG), "Airplane Strength and Rigidity - Flight Loads," 18 May 1960.

4. MIL-A-8863A, "Airplane Strength and Rigidity - Ground Loads for Navy Procurred Airplanes," 12 July 1974.

5. MIL-A-8864, "Airplane Strength and Rigidity - Water and Handling Loads For Seaplanes," May 1960.

6. MIL-A08865(ASG), "Airplane Strength and Rigidity -Miscellaneous Loads," 18 May 1960.

7. MIL-A-8866(ASG), "Airplane Strength and Rigidity - Reliability Requirements, Repeated Loads, and Fatigue," 18 May 1960.

8. MIL-A-8867(ASG), "Airplane Strength and Rigidity - Ground Tests," 18 May 1960.

9. MIL-A-8868A, "Airplane Strength and Rigidity - Data and Reports," 8 February 1974.

10. MIL-A-8869, "Airplane Strength and Rigidity - Special Weapons Effects."

11. MIL-A-8870, "Airplane Strength and Rigidity - Vibration, Flutter and Divergence."

12. W. Breyan, "Effect of Block Size, Stress Level and Loading Sequence on Fatigue Characteristics of Aluminum-Alloy Box Beams," ASTM STP 462, 1970, pp. 127.

13. M. S. Rosenfeld, "Aircraft Structural Fatigue Research in the Navy," Symposium on Fatigue Tests of Aircraft Structures: Low-Cycle, Full-Scale and Helicopters, ASTM STP 338, 1962, pp. 216.

14. I. G. Hedrick, L. B. Wehle, and P. D. Bell, "Fatigue and Fracture Considerations for Tactical Aircraft," AGARD Conference Proceedings No. 141, Specialists Meeting on Design Against Fatigue, AGARD-CP-141, Dec. 1973, pp. 4-1 through 4-15.

REFERENCES (Continued)

15. R. W. Smith, M. H. Hirshberg, and S. S. Manson, "Fatigue Behavior of Materials Under Strain Cycling in Low and Intermediate Life Range," NASA TN-1574, April 1963.

16. E. Z. Stowell, "Stress and Strain Concentration at a Circular Hole in an Infinite Plate, NASA TN-2073, 1950.

17. H. Neuber, "Theory of Notch Stresses: Principles of Exact Stress Calculations," J. W. Edwards, Ann Arbor, Michigan, 1946.

18. T. Broom, A. J. Nicholson, Journal Inst. of Metals, 89, 183 (1960).

19. F. J. Bradshaw, C. Wheeler, Applied Materials Research, 5, 112 (1966).

20. C. Laird, G. L. Smith, Phil. Mag., 8, 1945 (1963).

21. N. J. Wadsworth, Phil. Mag., 6, 63, 397 (1961).

22. N. E. Frost, Applied Materials Research, 3, 131 (1964).

23. N. Thompson, N. J. Wadsworth, N. Lovat, Phil. Mag., 1, 113 (1956).

24. J. C. Grosskrevtz, C. O. Bowles, Env. Sensitive Mechanical Behavior, Eds. Westwood and Stoloff, Gordon and Breach (1967).

25. J. C. Grosskrevtz, Surface Science, 8, 173 (1967).

26. D. J. Duquette, M. Gell, AMRDL, P&WA, unpublished research (1970).

27. H. Smith, P. Shahinian, Trans. ASM, 62, 549 (1969).

28. J. A. Bennett, J. Res. NBS, 68C, 91 (1964).

29. H. Shen, S. E. Podlaseck, I. R. Kramer, Acta Met., 14, 341 (1966).

30. K. V. Snowden, Acta Met., 12, 265 (1964).

31. K. V. Snowden, J. N. Greenwood, Trans. AIME, October, 1958, p. 626.

32. N. J. Wadsworth, J. Hutchings, Phil. Mag., 3, 34, 1154 (1958).

33. M. J. Hordon, Acta Met., 14, 1173 (1966).

34. M. R. Achter, ASTM STP 415, 181 (1967).

REFERENCES (Continued)

35. R. M. Latanasian, A.R.C. Westwood, Advances in Corrosion Science and Technology, Plenum Press, 80 (1967).

36. A. J. Gould, Engineering 136, A53 (1933).

37. A. J. Gould, Engineering 141, 495 (1936).

38. D. J. McAdam, Jr., Proc. ASTM 28, 117 (1928).

39. D. J. McAdam, Jr., Proc. ASTM 31, 259 (1931).

40. I. Cornet, S. Golan, Corrosion 15, 262t (1959).

41. D. J. McAdam, Jr., G. W. Geil, Proc. ASTM 41, 696 (1941).

42. B. B. Westcott, Mechanical Engr. 60, 813 (1938).

43. K. V. Snowden, J. of Less-Common Metals, 7, 84 (1964).

44. I. S. Shaffer, J. C. Sebastian, M. S. Rosenfeld, S. J. Ketcham, Journal of Materials, MJLSA, Vol. 3, No. 2, 400 (1968).

45. M. T. Chorabji Simnad, U. R. Evans, VISI, 156 (1947).

46. D. J. Duquette, H. H. Uhlig, Trans. ASM, 62, 839 (1969).

47. D. J. Duquette, H. H. Uhlig, Trans. ASM, 61, 449 (1968).

48. U. R. Evans, M. T. Simnad, Proc. Roy. Soc. A188, 372 (1947).

49. K. Laute, Oberfalchentech, 10, 281 (1933).

50. A. V. Ryabchenkov, Zhui, Fiz. Khim., 26, 542 (1952).

51. H. Spahn, Metalloberflache, 16, 369 (1962).

52. H. Spahn, Z. Physik. Chem. (Liepzig), 234, 1 (1967).

53. C. Laird, D. J. Duquette, Corrosion Fatigue, NACE-2, 346 (1972).

54. D. Whitman, U. R. Evans, JISI 165, 72 (1950).

55. H. N. Hahn, D. J. Duquette, Acta Met., 26, 279 (1978).

REFERENCES (Continued)

56. H. Masuda, D. J. Duquette, Met. Trans. 6A, 87 (1975).

57. U. R. Evans, The Corrosion and Oxidation of Metals, Edward Arnold, Ltd., London (1960).

58. F. Lohl, Metall., 4, 130 (1950).

59. L. Glikman, L. Suprun, Trudy Vsesoyoz Soveschenlya Po Boibe Smorskoi Korroziei Metal, Baku, 102 (1956).

60. M. E. Fine and R. O. Ritchie, "Fatigue Crack Initiation and Near-Threshold Crack Growth," Fatigue and Microstructure, 1978 ASM Materials Science Seminar, American Society for Metals, Oct. 1978, pp. 245.

61. C. Laird, Fatigue and Microstructure, 1978 ASM Materials Science Seminar, American Society for Metals, Oct. 1978, pp. 245.

62. M. E. Fine, Met. Trans A, Vol. 11A, No. 3, March, 1980, pp. 365.

63. D. J. Duquette, Fatigue and Microstructure, ASM, 335 (1978).

64. Y. H. Kim, "Initiation and Growth of Fatigue Microcracks and Strain-Controlled Fatigue Properties in Steel Alloys: Microstructure and Mechanics," Ph.D. Thesis, Northwestern Univ., Evanston, Illinois, 1979.

65. Y. H. Kim, M. E. Fine and T. Mura, Met. Trans. A, Vol. 9A, 1978, pp. 1679.

66. Y. H. Kim, M. E. Fine and T. Mura: "Fatigue Crack Initiation: Theory," presented at AIME 109th Annual Meeting, Las Vegas, NV., Feb. 1980.

67. Y. H. Kim and M. E. Fine: "Theoretical Prediction of the Number of Cycles to Fatigue Crack Initiation due to the Irreversible Slip Step Formation," to be published in Met. Trans., (1982).

68. Y. H. Kim, M. E. Fine and T. Mura, Eng. Fract. Mech. Vol. 11, 1979, pp. 653.

69. L. F. Coffin, Jr., and J. F. Tavernelli, Trans. Met. Soc., AIME, Vol. 215, Oct. 1959, pp. 794.

70. S. S. Manson, "Fatigue: A Complex Subject - Some Simple Approximations," Experimental Mechanics, July 1975, pp. 1.

71. R. W. Landgraf, M. R. Mitchell and N. R. Pointe, "Monotonic and Cyclic Properties of Engineering Materials," Ford Motor Co. Tech. Report, Dearborn, Michigan, 1972.

REFERENCES (Continued)

72. J. M. Barsom, "Fatigue Crack Growth Under Variable Amplitude Loading in ASTM A514 Grade B Steel, ASTM STP 536, American Society for Testing and Materials, Philadelphia, 1978.

73. S. T. Rolfe and J. M. Barsom, Fracture and Fatigue Control in Structures, Prentice-Hall Inc., Englewood Cliffs, New Jersey (1977).

74. N. E. Dowling, "Fatigue Failure Predictions for Complicated Stress-Strain Histories," J. Materials, Vol. 7, No. 1, 1972, pp. 71.

75. G. H. Jacoby, ASTM STP 462, 1970, pp. 184.

76. J. Morrow and G. M. Sinclair, ASTM STP 237, Symposium on Basic Mechanisms of Fatigue, ASTM, 1958, pp. 83.

77. P. N. Thielen and M. E. Fine, Met. Trans. A Vol. 6A, 1975, pp. 2133.

78. S. I. Kwun, "Fatigue Behavior of Quenched and Tempered N6-Bearing HSLA Steel," Ph.D. Thesis, Marquette Univ., Milwaukee, Wisconsin, 1978.

79. E. A. Starke, Jr. and G. Lutjering, Fatigue and Microstructure, 1978 ASM Materials Science Seminar, American Society for Metals, Oct. 1978, pp. 205.

80. H. M. Press et al, "A Re-evaluation of Data on Atmospheric Turbulence and Airplane Gust Loads for Application in Spectral Calculations," NACA Report 1272, 1956.

81. S. D. Manning, G. H. Lemon, M. E. Waddoups and R. T. Achard, "Composite Wing for Transonic Improvement - Structural Reliability Studies," Vol. III, AFFDL-TR-71-24, Nov. 1972.

82. J. P. Gallagher and R. P. Wei, Corrosion Fatigue, NACE-2 (1972) pp. 409-423.

83. A. J. McEvily and R. P. Wei, Corrosion Fatigue, NACE-2 (1972) pp. 381-395.

84. R. P. Wei, Engineering Fracture Mechanics 1 (1970) pp. 633-651.

85. M. O. Speidel, M. J. Blackburn, T. R. Beck and J. A. Feeney, Corrosion Fatigue, NACE-2 (1972) pp. 324-345.

86. H. L. Marcus, J. C. Williams and N. E. Paton, Corrosion Fatigue, NACE-2 (1972) pp. 346-358.

87. W. E. Krupp, D. W. Hoeppner, and E. K. Walker, Corrosion Fatigue, NACE-2 (1972) pp. 468-483.

REFERENCES (Continued)

88. D. J. Duquette, Environment-Sensitive Fracture of Engineering Materials (Ed.: Z. A. Foroulis), TMS-AIME, p. 521.

89. D. J. Duquette, Fatigue and Microstructure (Ed.: M. Meshii), ASM Materials Science Seminar, ASM (1978), pp. 335-363.

90. H. L. Marcus, Fatigue and Microstructure (Ed.: M. Meshii), ASM Materials Science Seminar, ASM (1978), pp. 365-383.

91. Corrosion Fatigue, NACE-2, (Ed.: O. F. Devereux, A. J. McEvily and R. W. Staehle), 1972.

92. Fatigue Crack Propagation, ASTM-STP-415 (1967).

93. Fatigue and Microstructure (Ed.: M. Meshii), 1978 ASM Materials Science Seminar, ASM (1978).

94. Environment-Sensitive Fracture of Engineering Materials (Ed.: Z. A. Foroulis), TMS-AIME (1978).

95. Environmental Degradation of Engineering Materials (Ed.: M. R. Loutham, Jr. and R. P. McNitt), Virginia Polytechnic Inst., & NSF, (1977).

96. Effects of Environment and Complex Load History on Fatigue Life (Ed.: M. S. Rosenfled), ASTM-STP-462 (1968).

97. Stress Corrosion-New Approaches (Ed.: H. L. Craig, Jr.), ASTM-STP-610 (1975).

98. Fracture Mechanics (Ed.: C. W. Smith), ASTM-STP-677 (1978).

99. A. J. Kennedy, Processes of Creep and Fatigue in Metals, John Wiley & Sons, Inc., New York (1963).

100. P. G. Forrest, Fatigue of Metals, Pergamon Press (1962).

101. F. J. Bradshaw and C. Wheeler, RAE Tech. Rep. No. 68041 (1968).

102. A. Hartman, F. J. Jacobs, A. Nederveen and R. DeRijk, NRL Tech. Note No. M.2182 (1967).

103. S. J. Hudak and R. P. Wei, Corrosion Fatigue, NACE-2 (1972) pp. 433-434.

104. R. P. Wei, International J. Fracture Mechanics, 4 (1968) pp. 159-170.

REFERENCES (Continued)

105. F. J. Bradshaw and C. Wheeler, International J. Fracture Mechanics, Vol. 5, No. 4 (1969).

106. R. J. Selines and R. M. Pelloux, "Effect of Cyclic Stress Wave Form on Corrosion Fatigue Crack Propagation in Al-Zn-Mg Alloys," MIT, Cambridge, Mass., (1972).

107. F. J. Bradshaw and C. Wheeler, Applied Materials Research, Vol. 5, No. 2 (1966).

108. J. M. Barsom, Corrosion Fatigue, NACE-2 (1972), pp. 424-436.

109. J. M. Barsom and S. R. Novak, NCHRP 12-14, National Cooperative Highway Research Program, Washington, Sept. 1974.

110. J. P. Gallagher, NRL Report 7064 (1970).

111. G. A. Miller, S. J. Hudak and R. P. Wei, J. of Testing and Evaluation, 1 (1973), pp. 524-531.

112. J. M. Barsom, J. of Engineering Fracture Mechanics, 3 (1971).

113. J. P. Gallagher, J. of Materials, JMLSA, ASTM 6 (1971) p. 941.

114. R. P. Wei, P. M. Talda and C. Y. Li, Fatigue Crack Propagation, ASTM-STP-415 (1967), pp. 460-480.

115. G. A. Miller, S. J. Hudak and R. P. Wei, J. of Testing and Evaluation, ASTM 1 (1973), pp. 524-530.

116. R. P. Wei and J. D. Landes, International J. Fracture Mechanics, 5 (1969) pp. 69-71.

117. R. P. Wei and M. O. Speidel, Corrosion Fatigue, NACE-2 (1972), pp. 379-380.

118. R. P. Wei and G. W. Simmons, Stress Corrosion Cracking and Hydrogen Embrittlement of Iron Base Alloy, NACE-5 (1977), pp. 751-765.

119. R. P. Wei, J. of Engineering Fracture Mechanics, 1 (1970), p. 633.

120. R. P. Wei and J. D. Landes, Materials Research and Standards, 9 (1969), pp. 25-28.

121. C. R. Saff, "Environment-Load Interaction Effects on Crack Growth in Landing Gear Steels," NADC-79095-60, (1980) McDonnell Aircraft Co., St. Louis, MO.

REFERENCES (Continued)

122. H. D. Dill and C. R. Saff, "Environment-Load Interaction Effects on Crack Growth," AFFDL-TR-78-137 (1978), McDonnell Aircraft Co., St. Louis, MO.

123. C. R. Saff and M. S. Rosenfeld, "Load-Environment Interaction Effects on Crack Growth in Landing Gear Steels," presented in 14th National Symposium on Fracture Mechanics, Los Angeles, CA (1981).

124. R. P. Wei and G. W. Simmons, ONR Contract No. N00014-75-C-0543, NR 036-097 (1979).

125. R. P. Wei, "Rate Controlling Processes and Crack Growth Response," presented at the Third Int. Conf. Effect of Hydrogen on Behavior of Materials," Jackson Lake, WY, (1980).

126. G. W. Simmons, P. S. Pao and R. P. Wei, Met. Trans. A, 9A (1978), pp. 1147-1158.

127. D. J. Dwyer, G. W. Simmons and R. P. Wei, Surface Science, 64 (1977), pp. 617-632.

128. R. P. Wei and G. W. Simmons, Scripta Metallurgica, 10 (1976), pp. 153-157.

129. P. S. Pao, W. Wei and R. P. Wei, Environment-Sensitive Fracture of Engineering Materials (Ed.: Z. A. Foroulis) TMS-AIME (1978), pp. 565-580.

130. M. Lu, P. S. Pao, T. W. Weir, G. W. Simmons and R. P. Wei, Met. Trans. A, 12A (1981) pp. 805-811.

131. R. L. Brazill, G. W. Simmons and R. P. Wei, J. of Engineering Materials and Technology, Trans. ASME, 101, 3 (1979) pp. 199-204.

132. Y. H. Kim and S. D. Manning, "A Superposition Model for Corrosion Fatigue Crack Propagation in Aluminum Alloys," presented in the 14th National Symposium on Fracture Mechanics, Los Angeles, CA (1981).

133. R. P. Wei and G. W. Simmons, International J. Fracture, 17 (1981), pp. 235-247.

134. R. P. Wei, P. S. Pao, R. G. Hart, T. W. Weir and G. W. Simmons, Met. Trans. A, 11A (1980), pp. 151-158.

135. R. J. Jacko and D. J. Duquette, "The Role of Hydrogen on Environmental Fatigue of High Strength Aluminum Alloys," Tech. Rep., the Office of Naval Research, Cont. No. N00014-75-C-0466, NR 036-093 (1980).

136. P. Shahinian and K. Sadanada, "Environmental Effects on Fatigue Behavior of Metals," Tech. Rep., NRL Memorandum Report 4495 (1981).

REFERENCES (Continued)

137. R. P. Wei, N. E. Fenelli, K. Unangst and T. T. Shih, J. of Engineering Materials and Technology, ASME Trans. Ser. H, Vol. 109 (1980) pp. 280-292.

138. G. R. Chanani, ASTM-STP-642 (1978), pp. 51-73.

139. Load and Environment Interactions in Fatigue Crack Growth, Proceedings - Int. Conf. Prospects of Fracture Mechanics, Delft, Netherlands, (1974), pp. 231-248.

140. J. W. Hagemeyer, "Overload Induced Retardation of Fatigue Cracks in Several Aluminum and Titanium Alloys," ERR-FW-1779, GD/FWD (1976).

141. O. E. Wheeler, "Spectrum Loading and Crack Growth," J. of Basic Eng. ASME, Vol. 94, Sec. D, No. 1, March 1972, pp. 181.

142. J. P. Gallagher, "A Generalized Development of the Yield Zone Materials," AFFDL-TM-FBR-74-28, Jan. 1974.

143. J. D. Willenborg, R. M. Engle, Jr. and H. A. Wood, "A Crack Growth Retardation Model Using Effective Stress Concepts," AFFDL-TM-71-1-FBR, Jan. 1971.

144. J. P. Gallagher and T. F. Hughes, "Influence of Yield Strength on Overload Affected Fatigue Crack Growth Behavior in 4340 Steel," AFFDL-TR-74-27, July 1974.

145. W. Elber, "The Significance of Fatigue Crack Closure," ASTM STP 486, 1971, pp. 230-242.

146. J. B. Chang, "Improved Methods for Predicting Spectrum Loading Effects," AFFDL Cont. No. F33615-77-C-3121, Final Report (1981).

147. H. D. Dill and C. R. Saff, ASTM-STP-595, (1976), pp. 306-319.

148. K. Walker, ASTM-STP-462 (1968), pp. 1-14.

NON-GOVERNMENT ACTIVITIES

	No. of Copies
ALCOA, ALCOA Labs, ALCOA Center, PA 15069 (Attn: Mr. J. G. Kaufman)	1
Battelle Columbus Labs, 505 King Avenue, Columbus, OH 43201 (Attn: Dr. B. Leis)	1
Boeing Commercial Airplane Co., P. O. Box 3707, Seattle, WA 98124 (Attn: Mr. T. Porter)	1
Douglas Aircraft Co., 3855 Lakewood Blvd., Long Beach, CA 90846 (Attn: Mr. Luce, Mail Code 7-21)	1
Drexel University, Phila., PA 19104 (Attn: Dr. Averbuch)	1
Fairchild Industries, Hagerstown, MD 21740 (Attn: Tech. Library)	1
General Dynamics, Convair Division, San Diego, CA 92138 (Attn: Mr. G. Kruse)	1
General Dynamics Corporation, P. O. Box 748, Ft. Worth, TX 76101 (Attn: Dr. S. Manning)	1
Grumman Aerospace Corporation, South Oyster Bay Road, Bethpage, L.I., NY 11714 (Attn: Dr. H. Armen)	
(Attn: Dr. B. Leftheris)	1
(Attn: Dr. H. Eidenoff)	1
Lehigh University, Bethlehem, PA 18015	
(Attn: Prof. G. C. Sih)	1
(Attn: Prof. R. P. Wei)	1
Lockheed-California Co., 2555 N. Hollywood Way, Burbank, CA 91520 (Attn: Mr. E. K. Walker)	1
Lockheed Georgia Co., Marietta, GA 30063 (Attn: Mr. T. Adams)	1
McDonnell Douglas Corporation, St. Louis, MO 63166	
(Attn: Mr. L. Impellizeri)	1
(Attn: Dr. R. Pinckert)	1
Northrop Corporation, One Northrop Ave., Hawthorne, CA 90250	
(Attn: Mr. Alan Liu)	1
(Attn: Dr. M. Ratwani)	1
Rockwell International, Columbus, OH 43216 (Attn: Mr. F. Kaufman)	1
Rockwell International, Los Angeles, CA 90009 (Attn: Mr. J. Chang)	1
Rockwell International Science Center, 1049 Camino Dos Rios, Thousand Oaks, CA 91360 (Attn: Dr. F. Morris)	1
Rohr Corporation, Riverside, CA 92503 (Attn: Dr. F. Riel)	1
Sikorsky Aircraft, Stratford, CT 06622	1
University of Dayton Research Institute, 300 College Park Ave., Dayton, OH 45469 (Attn: Dr. J. Gallagher)	1
University of Illinois, College of Engineering, Urbana, IL 61801 (Attn: Dept. of Mechanics and Industrial Eng., Profs. J. D. Morrow, D. F. Socie)	2
Vought Corporation, Dallas, TX 75265	
(Attn: Dr. C. Dumisnil)	1
(Attn: Mr. T. Gray)	1
University of Pennsylvania, Dept. of Mechanical Engineering and Applied Mechanics, 111 Towne Bldg. D3, Phila., PA 19104 (Attn: Dr. Burgers)	1

FAA

	No. of Copies
FAA, Washington, DC 20591 (Attn: J. R. Soderquist)	1
FAA, Technology Center, Atlantic City, NJ 08405 (Attn: Mr. D. Nesterok, ACT-330)	1

NASA

NASA, Langley Research Center, Hampton, VA 23365 (Attn: Mr. H. Hardrath)	1
NASA, Washington, DC 20546 (Attn: Airframes Branch, FS-120)	1
NASA, Lewis Research Center, Cleveland, OH 44135 (Attn: Technical Library)	1
NASA, George C. Marshall Space Flight Center, Huntsville, AL 35812 (Attn: Technical Library)	1

USAF

AFWAL, WPAFB, OH 45433 (Attn: AFWAL/FIBE)	1
(Attn: FIBEC)	1
(Attn: FIBAA)	1
(Attn: AFWAL/FIB)	1
Ogden ALC, Hill AFB, UT 84055 (Attn: MANCC)	1
Oklahoma City ALC, Tinker AFB, OK 73145 (Attn: MAQCP)	1
Sacramento ALC, McClellan AFB, CA 95652 (Attn: MANE)	1
San Antonio ALC, Kelly AFB, TX 78241 (Attn: MMETM)	1
Warner Robbins ALC, Robins AFB, GA 30198 (Attn: MMSRD/Dr. T. Christian)	1

U. S. Army

Applied Technology Laboratory, USARTL (AVRADCOM), Fort Eustis, VA 23604 (Attn: H. Reddick)	1
U. S. Army Materials and Mechanics Research Center (DRXMR-PL), Watertown, MA 02172	1
U. S. Army Research Office, Durham, NC 27701	1

INFO. SERVICES

DTIC, Cameron Station, Alexandria, VA 22314	12
MCIC, Battelle Columbus Laboratories, 505 King Avenue, Columbus, OH 43201	1
NTIS, U. S. Dept. of Commerce, Springfield, VA 22151	2

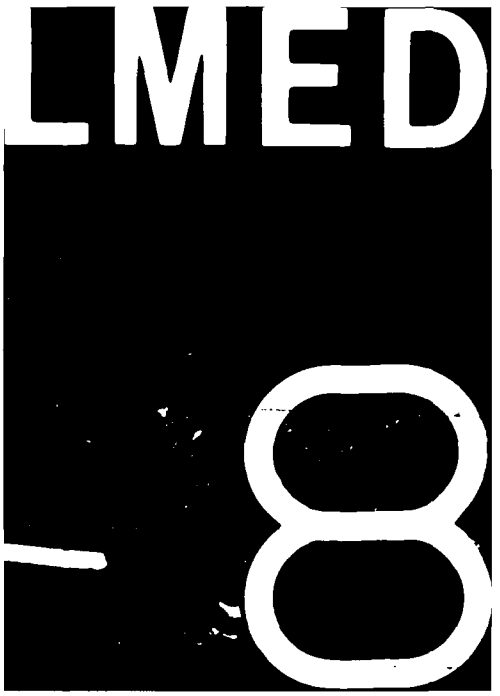
LMED
8